Rheology, mechanical properties, barrier properties of poly(lactic acid)

Violette Ducruet, Samira Fernandes Nassar, Sandra Domenek

Adv Polym Sci (2018) 279: 303–342
DOI: 10.1007/12_2016_17

Published online: 26 July 2017

Rheology, Mechanical Properties, and Barrier Properties of Poly(lactic acid)

Sandra Domenek, Samira Fernandes-Nassar, and Violette Ducruet

Abstract Knowledge of the fundamental parameters of the poly(lactic acid) (PLA) molecular chain and resulting macroscopic properties is important for successful application of this polymer in different domains. Rheological data show that PLA has the typical properties of a linear and semi-stiff polymer chain. The stereochemical composition of the atactic polymer chain does not impact the rheological, mechanical, and barrier properties of PLA. Most commercial PLA grades contain a large majority of L-lactic acid units, in which case the polymer is named PLLA. PLLA at room temperature is a brittle glassy polymer and its main fracture mechanism is crazing. Above the glass transition, semicrystalline PLLA shows extensive cavitation. Uniaxial deformation above, but near, the glass transition temperature leads to the formation of a mesophase, responsible for strain hardening. At higher temperatures, strain hardening is caused by induced crystallization. The PLLA oxygen barrier properties are comparable to those of polystyrene (PS). The water vapor barrier properties are higher than those of PS because of the higher polarity of the polymer chain. An increase in barrier properties can be obtained by specific crystallization techniques, multilayer strategies, or the addition of (nano) fillers.

Keywords Barrier properties • Biopolymer • Crystallization • Degradation • Mechanical properties • Packaging • PLA synthesis • Poly(lactic acid) • Poly (lactide) • Process

S. Domenek (✉), S. Fernandes-Nassar, and V. Ducruet
UMR Ingénierie Procédés Aliments, AgroParisTech, INRA, Université Paris-Saclay, 1 rue des Olympiades, 91300 Massy Cedex, France
e-mail: sandra.domenek@agroparistech.fr

Contents

1 Introduction

The objective of the present chapter is to summarize the fundamental and application-relevant properties of poly(lactic acid) (abbreviated PLLA when the L-lactic acid content is much greater than the D-lactic acid content). Rheology, in particular, gives insight into the fundamental characteristics of the macromolecular chain, which can be linked to its macroscopic features. The flexibility and physical dimensions of the macromolecular chain influence its entanglement capacity and, therefore, the melt viscosity and processing ability. Furthermore, mechanical properties such as high ductility are obtained when the macromolecular chains can accommodate deformation at the imposed time scale. The barrier properties are conditioned by the chemical structure of the polymer chain and the free volume present in the material. Understanding and control of those parameters are key for the successful application of PLLA in different fields.

We would like to recall here some fundamentals on the structure of PLLA (more details can be found in other chapters of this book). PLLA is a semicrystalline polyester with a glass transition temperature (T_g) of around 60°C. The monomer of PLLA, lactide, has two chiral centers, which allows the synthesis of PLA macromolecules with different stereochemistries. Microbial production of lactic acid yields primarily the stereoisomer L-lactic acid, which is therefore the principal reactant for formation of the lactide ring. In this chapter, the stereochemistry of PLA will therefore be indicated by the molar percentage of the minor stereoisomer, D-lactic acid (% D), in the macromolecular chain. In cases where the stereochemistry of adjacent chiral centers in the macromolecule is controlled, the polymer chain presents specific tacticity, that is, specific orderliness of the succession of the configurational repeating units in the main chain (IUPAC definition). Briefly, in

isotactic macromolecules, all substituents are located on one side of the main chain. In PLA the substituent is the methyl group, and the isotactic polymer is composed of either 100% L-lactic acid or 100% D-lactic acid. In syndiotactic polymers, the substituents are alternately located at one and the other side of the main chain. In the case of PLA, the polymer could have, for example, an alternating structure of L-lactic acid and D-lactic acid units (L-D-L-D). Heterotactic polymers are constituted of a regular succession of diads or triads; for PLA the succession is DD-LL-DD-LL. In atactic polymers, the sequence of L- and D-lactic acids is not controlled. This is the case for most commercial polymers, where, in addition, the quantity of D-lactic acid in the chain is small (typically below 5 mol%). In some academic studies, however, the tacticity of PLA was controlled and, in these cases, the tacticity is specifically indicated in the text.

The proportion of D- and L-lactic acid units in the polymer chain has primary importance for the crystallization properties of PLA. The use of racemic proportions of PDLA and PLLA yields the formation of stereocomplexes that crystallize at temperatures different from the crystallization temperatures of the homopolymers. Furthermore, PLA presents a crystalline polymorphism. The most usual crystalline form is the α-polymorph, characterized by a left-handed 10_3 helix and a pseudo-orthorhombic or orthorhombic unit cell. At low crystallization temperatures (typically below 110°C), a disordered α-polymorph with larger unit cell dimensions is obtained. This polymorph was originally named the "α′-form," but recent literature proposes that it be renamed "δ-polymorph." In the present chapter, we will stick to the initial name and use the denomination "α′-form" for this polymorph.

2 Rheology of PLA

2.1 Solution Rheology

Garlotta [1] has presented an overview of PLA properties in solution, showing that there are conflicting data in the literature concerning solution rheology. In response, Dorgan et al. [2] investigated very systematically the fundamental properties of PLA using a multimethod strategy by comparing data from solution rheology, light scattering, and melt rheology. PLAs with 0 and 20% D-lactic acid and different chain lengths were synthesized and the solution rheology parameters analyzed in chloroform ($CHCl_3$), tetrahydrofuran (THF), and mixtures of dichloromethane (CH_2Cl_2) and acetonitrile (CH_3CN). Analysis of the intrinsic viscosity ($[\eta]$) of the macromolecules as a function of the solvent and the molecular weight averages (M) allowed the Mark–Houwink parameters (K and α) to be obtained with the help of the Mark–Houwink equation:

$$[\eta] = KM^{\alpha}. \tag{1}$$

t1.1 **Table 1** Mark–Houwink parameters for PLA in THF

t1.2 PLA sample	Mark–Houwink fit		Reference
	K (mL/g)	α	
t1.4 Pooled data 0, 20, 50% D	0.0174 ± 0.0046	0.736 ± 0.023	[2]
t1.5 Commercial PLLA[a]	0.014	0.75	[5]
t1.6 Atactic (different % D)	0.014	0.76	[6]
t1.7 Isotactic (tacticity 0.71)	0.015	0.76	[3]
t1.8 Heterotactic (tacticity 0.96)	0.010	0.76	[3]
t1.9 Heterotactic (tacticity 0.60)	0.011	0.76	[3]
t1.10 Syndiotactic (tacticity 0.72)	0.009	0.76	[3]

t1.11 [a]The authors used different types of PLLA purchased from NatureWorks and pooled the data obtained
K Mark–Houwink front factor, α Mark–Houwink exponent

The Mark–Houwink parameters depend on the polymer–solvent system, where the exponent α is characteristic for the solvent quality and polymer flexibility. The value $\alpha = 0.5$ indicates a theta solvent. A high value, such as $\alpha = 0.8$, indicates a good solvent and a stiff polymer chain. Dorgan et al. [2] showed that the relative percentage of the optical co-monomers in the PLA chain did not impact the fundamental rheological parameters. The Mark–Houwink plot of PLA was linear, which implies that PLA behaves as a linear polymer with random coil conformation in the tested solvents. Table 1 gives the solution rheology constants of PLA in THF. The exponents of the Mark–Houwink plot were between 0.5 and 0.8, which shows good-solvent conditions. Chile et al. [3] studied PLA with controlled tacticity and concluded that only the isotactic chain of PLA developed higher $[\eta]$ than the other types of tacticity (compare entries for isotactic and other PLA samples in Table 1). The creation of branched and star-like structures decreased $[\eta]$ of PLA [4] compared with the linear polymer chain of equivalent molecular weight. The value of $[\eta]$ decreased from 35.7 mL/g (linear chain M_w 1.97 × 10^3, solvent $CHCl_3$) to 24.2 mL/g (star-shaped chain M_w 1.94 × 10^3).

The characteristic ratio (C_∞) of the unperturbed polymer chain in dilute solution was calculated from the Stockmayer–Fixman fit of $[\eta]$ for the acquisition of the front factor K_Θ in several common solvents [2]. The front factor describes the unperturbed chain dimensions in dilute solution and can be obtained from the Mark–Houwink fit in theta conditions. The Stockmayer–Fixmann fit is a means to retrieve K_Θ. It reads:

$$\frac{[\eta]}{M^{1/2}} = K_\Theta + bM^{1/2}, \tag{2}$$

where b is a solvent-dependent factor. The front factor can depend slightly on temperature, but is independent of solvent. With the help of K_Θ, C_∞ can be calculated:

$$C_\infty = \left(\frac{K_\Theta}{\Phi}\right)^{2/3} M_l/\overline{l^2}, \tag{3}$$

Table 2 Dilute solution constants for PLA (pooled data of PLA with 0, 20 and 50% D), adapted from [2]

Solvent	Parameter	$CHCl_3$	THF	CH_3CN/CH_2Cl_2
Mark–Houwink fit	K (mL/g)	0.0131 ± 0.0048	0.0174 ± 0.0046[a]	0.0182 ± 0.0075
	α	0.777 ± 0.031	0.736 ± 0.023[a]	0.697 ± 0.034
Stockmayer–Fixman fit	K_Θ (mL/g)	0.112 ± 0.017	0.101 ± 0.014	0.096 ± 0.011
	b (10^4)	5.82 ± 0.69	4.76 ± 0.65	2.30 ± 0.36
	C_∞	6.74 ± 0.67	6.29 ± 0.57	6.08 ± 0.46

[a]For comparison, data are repeated from Table 1

K, α Mark-Houwink parameters, K_Θ, b Stockmayer-Fixman parameters, C_∞ characteristic ratio

with Φ being the Flory constant (2.55×10^{23}), M_1 the relative molar mass per backbone bond (24.02), and $\overline{l^2}$ the mean squared backbone length (2.05 Å^2) of PLA. C_∞ is a measure of chain rigidity, as it corresponds to the ratio of the mean squared end-to-end distance of the freely joined chain ($<R^2>$) over the sum of the squared segment length ($N\overline{l^2}$), $C_\infty = \frac{\langle R^2 \rangle}{N\overline{l^2}}$. The C_∞ value for an ideal random chain would be equal to one; the higher the value of C_∞, the stiffer the polymer chain. The corresponding data are given in Table 2.

Several authors have measured the dependence of the hydrodynamic radius (R_h) of PLLA on the molecular weight using the solvent THF [5, 6]. The relationships obtained were $R_h = 0.017 M_W^{0.56}$ and $R_h = 0.016 M_W^{0.56}$, which are typical for random coil polymers in good solvent. The influence of tacticity on the scaling relationship seemed to be negligible, except maybe a small effect for the isotactic sample [3].

2.2 Melt Rheology

To understand the PLLA processing ability and flow in melt processes, analysis of the viscoelastic behavior as a function of temperature is useful. Master curves of the viscoelastic behavior of PLLA spanning from the glass to the melt can be obtained by applying the time–temperature superposition principle. The viscoelastic moduli of a polymer depend on the measurement frequency and temperature. If the measurement frequency is sufficiently low, the characteristic times for polymer relaxation are shorter than the measuring time and the viscous character of the polymer is preponderant. At high frequencies, polymer relaxation can only occur at small length scales and the elastic character is thus dominant. This interdependency can be used to obtain master curves of the viscoelastic behavior of polymers over a wide range of temperature and frequency by shifting isothermal frequency sweep curves with the help of shift factors. The laws of Williams–Landel–Ferry (WLF) and Arrhenius establish the equivalence between the frequency (time) and the temperature. The WLF equation applies to long-range relaxation movements, whereas the Arrhenius equation applies to local relaxations. One of the difficulties

in measuring the viscoelastic behavior of PLA is the low thermostability of the polymer, which results in degradation during rheological measurement in the melt. Therefore, the data for PLA often fail to comply with the time–temperature superposition principle. Palade et al. [7] developed a method, now often employed, using tris(nonylphenyl)phosphite (TNPP) as stabilizer to suppress thermo-hydrolysis of PLA.

A typical master curve of the linear viscoelasticity of PLA is shown in Fig. 1 [6]. The vertical shift factors used for its construction ranged from 0.98 to 1.03, which is consistent with values for linear polymers [8]. The horizontal shift factors followed the law of Arrhenius and were independent of molecular weight. The activation energy of flow was 177 kJ/mol. The terminal zones approached the typical slopes of 1 and 2 Pa s, which are predicted by the scaling relationships. Table 3 summarizes the viscoelastic plateau moduli (G_N^0), measured by several authors. The pooled data for atactic PLA showed that the quantity of D-lactic acid did not seem to correlate with the measured plateau modulus and entanglement length (M_e). However, the tacticity of the macromolecular chain seemed to have some influence on the parameters, where the sydiotactic polymer showed a lower stiffness and a higher entanglement length.

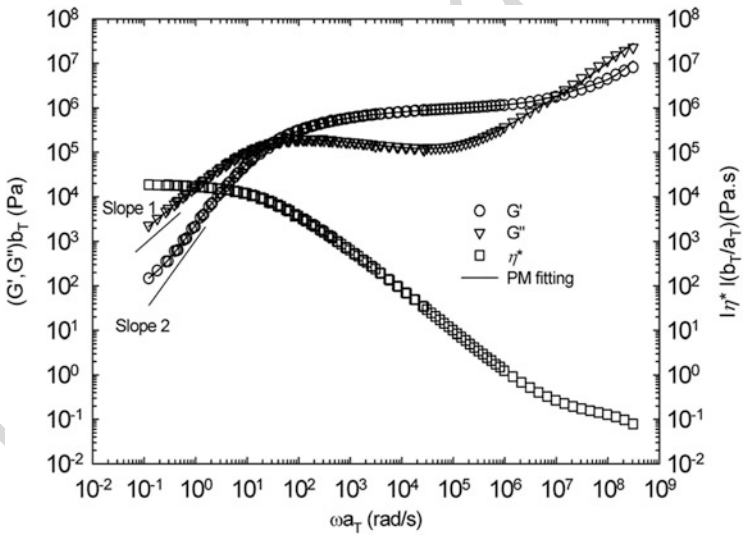

Fig. 1 Master *curve* of the linear viscoelastic moduli, G' and G'', and the complex viscosity (η^*) of PLA (50% D) at the reference temperature 150°C. Reproduced with permission from Othman et al. [6], Journal of Rheology, AIP Publishing LLC

Table 3 Viscoelastic properties of PLA melts t3.1

PLA sample	M_w (g/mol)	T (°C)	$G_N^0 \times 10^5$ (Pa)	M_e (g/mol)	Reference
4% D	750,000	180	5		[7]
50% D	165,000	150	9 ± 2	4,400	[6]
2% D		180	5	8,700	[9]
0% D		200		10,500[a]	[10]
Pooled data, different % D		140	1	3,959	[2]
Heterotactic (60% tacticity)	172,000	150	0.58	6,900	[3]
Heterotactic (96% tacticity)	191,000	150	0.52	7,700	[3]
Syndiotactic (86% tacticity)	150,000	150	0.34	11,800	[3]
Isotactic (71% tacticity)	123,000	150	0.97	4,100	[3]

[a]Estimated with the help of the Stockmayer–Fixman fit and the characteristic ratio

G_N^0 viscoelastic plateau modulus, M_e entanglement length

The dimensions of the linear PLA chains in the melt were characterized in detail by Dorgan et al. [2]:

- Mean-squared backbone length: 2.05 Å^2
- Flory constant Φ: 2.55×10^{23}
- Mean-squared radius $\left\langle r_0^2 \right\rangle \Big/ M$: 0.574 Å^2
- Critical entanglement length M_c: 9,211 g/mol (383 backbone bonds)
- Characteristic ratio C_∞: 6.7 ± 0.7 (140°C)
- Packing length p: 2.51 Å
- Tube diameter d_t: 47.7 Å

The C_∞ of PLA obtained from the melt is consistent with the value measured in solution. In the melt, PLA is therefore a highly flexible polymer, comparable to other linear polymers such as polyethylene oxide ($C_\infty = 5.6$) or isotactic polypropylene ($C_\infty = 6.2$) [11]. No influence of the optical co-monomer composition on C_∞ was found within experimental uncertainty, although theoretical analysis predicted some small influence [12].

PLA melts are non-Newtonian fluids, exhibiting shear thinning at high shear rates. The zero-shear viscosity was determined from the measurement of viscosity in the limit of low frequencies, with zero-shear viscosity values typically in the range of 10^2–10^4 Pa s for typical commercial polymers (M_w 140–160 kg/mol) (see Table 4). A summary of the data collected on the relationship between zero-shear viscosity and molecular weight is given in Table 4. Most of the power indexes given in recent literature correspond to the theoretical value of 3.4 for truly random materials. The pre-exponential factors (K_η) were rather low, which reflects low melt viscosity. The scaling law was independent of the optical composition of heterotactic and atactic polymers, within measurement uncertainty. However, the tacticity of the macromolecules had some impact on the melt rheology, where isotactic PLA had higher zero-shear viscosity and syndiotactic PLA lower zero-shear viscosity than heterotactic PLA [3]. Semicrystalline PLLA had a slightly higher melt viscosity than amorphous PLLA [13]. However, the PLLA melt

t4.1 **Table 4** Scaling relationships between zero-shear viscosity (power law $|\eta_0| = K_\eta \cdot M_W^n$) and molecular weight of amorphous PLA

t4.2 PLA sample	T_{ref} (°C)	$K_\eta \times 10^{-14}$ (Pa s)	n	Reference
t4.3 0% D	180	0.23	3.7	[16]
t4.4 Pooled data (0, 20, 50, 100% D)	180	0.550	3.4	[11]
t4.5 Pooled data (0, 10, 25, 50, 100% D)	150	6.31	3.4	[6]
t4.6 Heterotactic (60 and 86% tacticity)[a]	150	6.31	3.4	[3]
t4.7 Syndiotactic (86% tacticity)	150	1.65	3.4	[3]
t4.8 Isotactic (71% tacticity)	150	14.3	3.4	[3]

t4.9 K_η pre-exponential factor, n power index, T_{ref} reference temperature
[a]Chile et al. [3] used Othman's [6] parameters for the description of their heterotactic samples

207 viscosity and melt strength were low, which is a drawback for its application in the
208 fields of foaming and film extrusion [14–18]. A number of methods were experi-
209 mentally tested for increasing both properties, such as blending and use of in situ
210 crosslinking by various peroxides or epoxides during processing [14–18]. Peroxides
211 induce branching of PLLA chains, which increases the zero-shear melt viscosity
212 [14, 16]. However, branched polymers showed higher shear thinning in the high
213 frequency range [16]. Analysis of branched PLLA chains having a controlled
214 molecular structure (two-arm or three-arm branching or a mix of two-arm and
215 three-arm branched macromolecules) confirmed the positive impact of branching
216 on the zero-shear viscosity [19]. Stereocomplex technology can also help to
217 increase the PLA melt viscosity [20]. The connection between stereocomplexed
218 domains could be varied from chain entanglement to direct molecular bridging by
219 changing the content of stereocomplex (from 10 to 23%). Both the stereocomplex
220 crystals and the crosslinked network reinforced the PLA matrix, resulting in an
221 increase in melt viscosity [20].
222 The Cox–Mertz rule, which states the equivalence of dynamic and steady shear
223 viscosities, was shown to be valid for PLLA with different optical co-monomer
224 compositions (2 and 4% D) over a very wide viscosity range, extending into the
225 shear thinning region [7].

226 *2.3 Extensional Rheology and Melt Strength*

227 The extensional rheology of PLLA showed good superposition with the linear
228 viscoelastic envelope at low Hencky strain rates, where Hencky strain = ln
229 (length/(initial length)). At higher Hencky strain rates (from 1 to 10 s^{-1}) a shear
230 hardening effect was found for PLLA at various D-lactic acid contents (2, 4, and
231 50%) [6, 7]. The shear hardening effect faded at high temperatures. Analysis of
232 stretched PLLA melts showed the absence of stress-induced crystallization. Strain
233 hardening occurred when the longest relaxation times of the polymer chains were
234 longer than the characteristic times of deformation. This was caused by the pres-
235 ence of a long-chain tail in the PLLA molecular weight distribution. The behavior
236 could be successfully predicted by the Kaye–Bernstein–Kearsley–Zapas (K–BKZ)

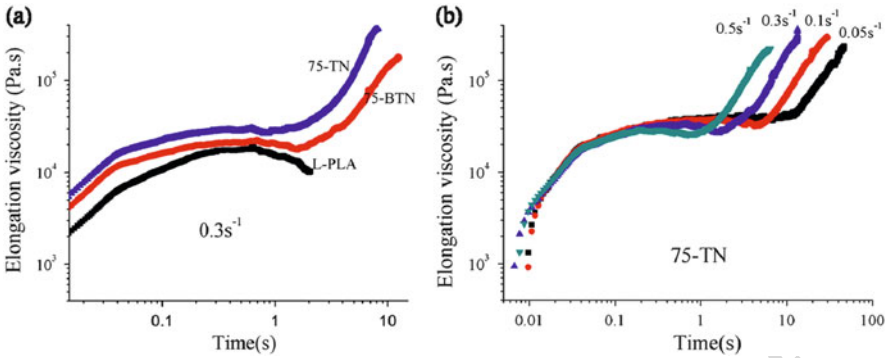

Fig. 2 Elongational viscosity as a function of time for (**a**) linear PLLA and long chain branched PLLA (*75-TN* three-arm branch with DP 75; *75-BTN* two-arm and three-arm branch with DP 75) at an elongational rate of 0.3 s^{-1} and (**b**) 75-TN at different elongational rates at 180°C. Reprinted with permission from Wang et al. [19], Industrial & Engineering Chemistry Research. Copyright 2016 American Chemical Society

constitutive equation [6]. Furthermore, the molecular architecture influenced the onset time of strain hardening, as shown in Fig. 2 [19].

Dean et al. [14] investigated the efficiency of peroxides for increasing the PLLA melt strength by crosslinking. They measured the Gottfert Rheotens melt strength of PLLA modified with lauroyl peroxide and showed an increase in force from approximately 0.017 to 0.06 N when using 1% of lauroyl peroxide. Al-Itry et al. [17] worked with an epoxy-modified acrylic copolymer (Joncryl™) and used the Cogswell method to show the positive action of the chain extender on the PLLA melt strength. The elongational viscosity increased tenfold from approximately 25,000 to 225,000 Pa s (180°C) with the addition of 1% Joncryl™. They also showed the positive impact of Joncryl™ on the PLLA blow extrusion stability and the widening of the processing window. The use of Joncryl™ allowed both formation of large bubbles and high film take-up ratios.

2.4 Conclusion

PLLA is a linear and rather rigid polymer, which adopts a random coil structure in good solvents. The tacticity of the polymer main chain has a low influence on its parameters in solution and in the melt, with the exception of the isotactic structure. Indeed, isotactic structures, but also branched structures, showed increased melt viscosity. One of the drawbacks of PLLA is its low melt strength. In this context, the increase in melt viscosity by controlling the tacticity of the PLLA main chain and the creation of branched and star-like structures is one of the research directions that will be followed in the future. The second strategy is the use of polymer additives, such as crosslinkers, during PLLA processing. In this respect, improvements in the processing ability have been obtained and a number of chemical companies now provide specific additives for PLLA.

3 Mechanical Properties of PLLA

3.1 *Hot Drawing*

Hot drawing of PLLA (i.e., deformation at temperatures higher than T_g) corresponds generally to processing situations in fiber spinning or biaxial stretching during film drawing or bottle blowing. An example of the stress–strain curves of semicrystalline PLLA under hot drawing is given in Fig. 3. The curves show an initial linear slope, then a yield peak, subsequent lowering of the slope of the stress–strain curve, and finally the onset of strain hardening.

The primary damage mechanism in semicrystalline PLLA upon hot drawing is cavitation and crystalline lamella damage and slip [21]. Cavitation is the formation of nano- to micrometer-sized voids in the amorphous phase or at the interface of the amorphous and crystalline phases. It implies a volume change of the polymer. Cavities occur around the yield point and a macroscopic manifestation of the phenomenon is stress whitening [22]. Cavities have no internal structure, in contrast to crazes. They are therefore unable to transfer stresses and elongate in the load direction upon drawing [22]. Investigation of the behavior of PLLA under hot drawing showed that stretching temperatures near T_g (70°C) promoted the initiation of cavitation before yielding and favored destruction of the ordered lamellar structure with an increase in stretching strain [21]. The supposed mechanism is sketched in Fig. 4. The cavities appeared and extended perpendicular to the stretching direction before yielding. The amorphous phase was only stretched slightly in this case (Fig. 4a). At further stretching deformation, more cavities appeared and their orientation changed from perpendicular to parallel to the load direction (Fig. 4b). The crystalline lamellae fractured, which destroyed the ordered lamellar structure (Fig. 4c). At high stretching temperature (90°C, far from the glass

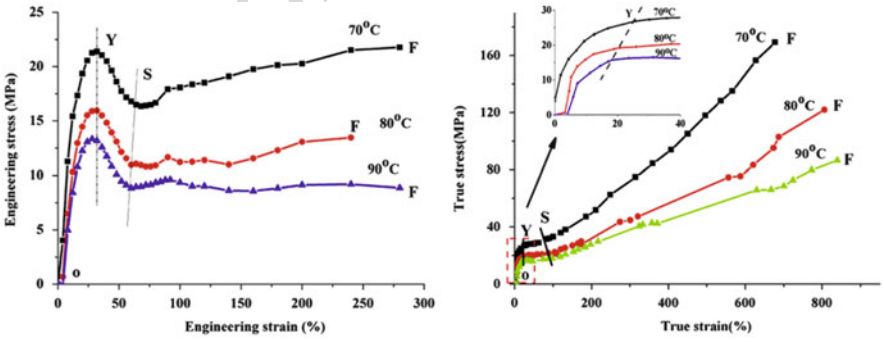

Fig. 3 Stress–strain *curves* for semicrystalline PLLA under hot drawing (crosshead speed 0.05 mm/s). The *left-hand* figure shows the engineering stress–strain plot obtained by a tensile testing machine and the *right-hand curve* the true stress–strain *curve* obtained by image correlation analysis of the deformation of a mesh grid printed on the test specimens. *Y* yield point, *S* beginning of strain hardening, *F* fracture. Reproduced with permission from Zhang et al. [21], Polymer, Elsevier

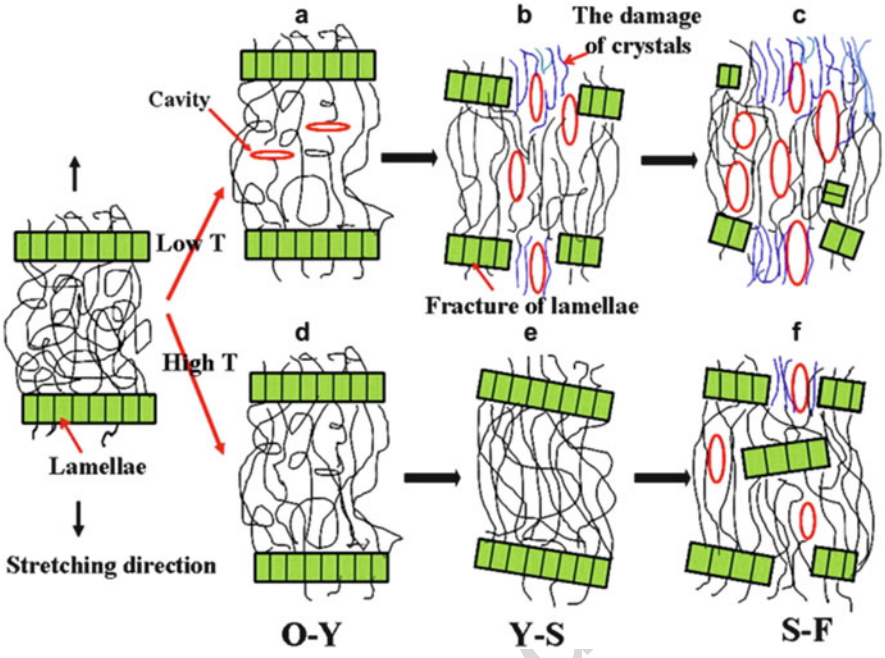

Fig. 4 Structure evolution of annealed PLLA with strain at different stretching temperatures. The low temperature conditions in Zhang's work were 70°C and the high temperature conditions 90°C. *O–Y* is the pre-yielding zone, *Y–S* the necking, and *S–F* the strain-hardening zone. Reproduced with permission from Zhang et al. [21], Polymer, Elsevier

transition), crystallite deformation and lamellae slip occurred without cavitation (Fig. 4d, e). In the strain-hardening zone, some orientated cavities along the stretching direction appeared and the lamellae fractured (Fig. 4f). The number and size of cavities and the imperfection of the lamellae are, however, smaller when the drawing temperature is higher [21].

Figure 5 (reproduced from [23]) shows a typical stress–strain curve for uniaxial drawing of initially amorphous PLLA. PLLA showed rubber-like behavior up to a critical strain level, which increased with the temperature. The yield peak, which was observed in the hot-drawing experiments using semicrystalline PLLA, was absent. Strain hardening occurred at the critical strain level and became softer at higher temperatures.

Two mechanisms can explain the occurrence of the strain-hardening phenomenon observed upon hot drawing of amorphous PLLA: (1) orientation-induced crystallization and (2) orientation of the amorphous phase. Analysis of the stretched PLLA samples showed that the drawing conditions governed the occurrence of either mechanism [24]. Figure 6 shows a phase diagram and sketch of the supposed molecular mechanisms in the case of molecular orientation and strain-induced crystallization [24]. At low drawing temperature or high drawing rates, entangled clusters are connected to each other by oriented and taut chains, which are not necessarily parallel. In that case, the experimental conditions did not allow

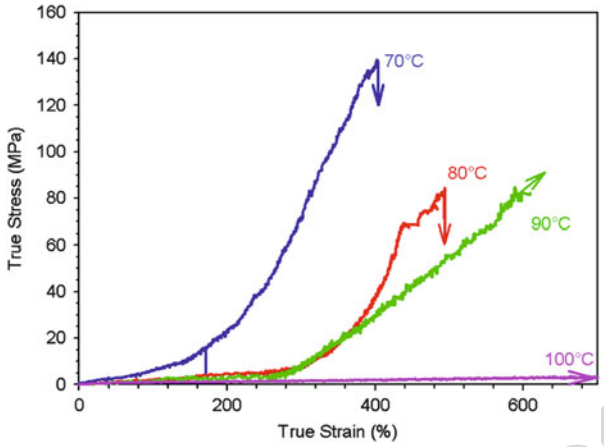

Fig. 5 True stress–strain *curves* for PLLA (4.3% D) films at different temperatures under uniaxial drawing (strain rate 0.04 s^{-1}, crosshead speed 50 mm/min). Reprinted with permission from Stoclet et al. [23], Macromolecules. Copyright 2016 American Chemical Society

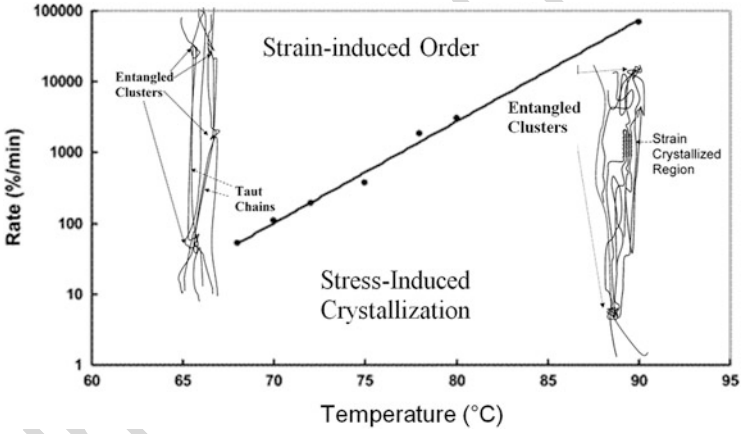

Fig. 6 Phase diagram for structure formation during uniaxial deformation of PLLA and sketch of the molecular deformation model. Adapted from Figures 17 to 19 of Mulligan et al. [24]

crystallization because of the lack of time for chain relaxation and arrangement in the crystallographic register. Mulligan et al. [24] interpreted this structure as nematic-like ordering. At higher temperatures or lower strain rates, the polymer chains, which were at intermediate orientation states, could crystallize as a result of adequate relaxation times (Fig. 6).

Stoclet et al. [23] shed novel light on the strain-induced ordering of amorphous PLLA chains upon drawing at temperatures above, but near to, T_g (70°C). With the help of in situ small-angle X-ray scattering (SAXS) experiments during uniaxial drawing, the authors showed the formation of a mesomorphic phase at the onset of

strain hardening. The mesomorphic phase was characterized by reduced interchain distance with regards to the spacing of the amorphous macromolecules. The higher cohesiveness of the mesomorphic domains generated physical crosslinking in the amorphous phase, leading to strain hardening. The mesomorphic phase was reported to be thermally stable up to 90°C. Upon drawing at intermediate temperatures (80°C), PLLA formed a mesomorphic phase and strain-induced crystallites. The ability of PLLA to form ordered phases (i.e., mesomorphic phase or crystallites) is directly linked to its stereoregularity. A critical value of 8% D was found, above which no ordering was induced, neither mesomorphic nor thermal, nor mechanically induced crystallization [25].

3.2 Cold Drawing

PLLA is a semicrystalline polymer and glassy at room temperature, therefore it presents brittle fracture behavior. The main deformation mechanisms of glassy polymers are crazing and shear banding. Crazing implies the formation of small voids (defects) in the amorphous phase, which are generally nucleated on surfaces. The voids are bridged by highly elongated fibrils and grow into crazes upon breakage of the fibrils. Crazes, in contrast to cavities, develop perpendicular to the draw direction, where the stress is concentrated on the edges. The formation of microvoids and crazes is also accompanied by volume change and begins around the yielding peak [26, 27]. Brittle fracture is finally caused by microcracks originating from breaking crazes [28]. The ductile behavior of polymer glasses exhibits yielding. Yield can be caused either by multiple crazes or by shear yielding (i.e., plastic flow without crazing). Whereas crazing occurs in materials at temperatures below T_g, shear yielding can be observed at a wide range of temperatures. The condition of shear yielding is that the critical shear stress for yielding is lower that the stress required to initiate and propagate crazes [28].

The second mechanism, shear banding, does not involve a polymer volume change. It consists in shear of the amorphous phase along slip planes that are oriented at approximately ±45° to the draw direction. The shear processes can be localized (fine slip) or diffuse (coarse slip). Slip occurs by the generation and propagation of dislocations between planes. A fine slip produces high deformation of the macromolecules and propagates quickly. In semicrystalline polymers, crystallographic fine slips cause the rotation of lamella planes in relation to the direction of the macromolecules. Therefore, fine slips cause rotation and thinning of the crystalline lamellae. Not much plasticity is created in that case and the fracture is brittle. Coarse slips are caused by the superposition of several fine slips. These slips propagate less quickly and produce more plasticity. The crystallographic coarse slips are responsible for the formation of block structures and lead to fragmentation of lamellae [22, 28].

Figure 7 presents typical stress–strain curves for tensile testing of PLLA (4.3% D) at different drawing temperatures [26]. At higher experimental temperatures, PLLA

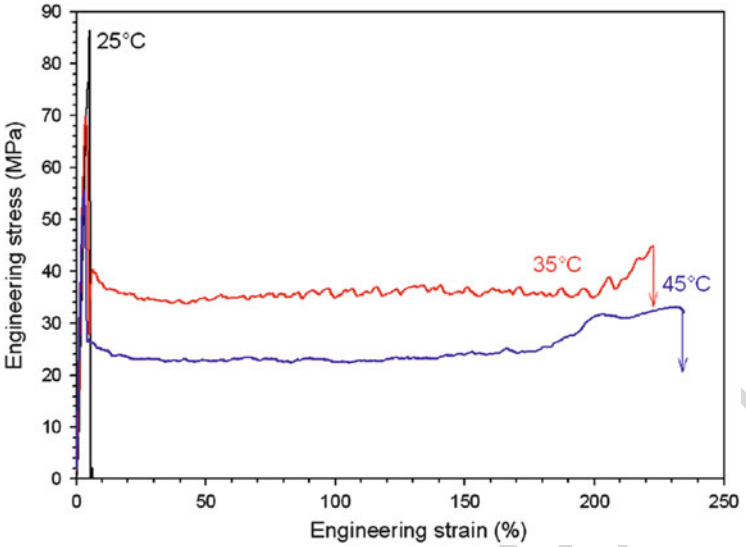

Fig. 7 Stress–strain *curves* for PLLA (4.3% D) drawn at different temperatures (strain rate 0.04 s^{-1}, $L_0 = 22$ mm, crosshead speed 52.8 mm/min). Reproduced with permission from Stoclet et al. [26], Polymer, Elsevier

showed ductile behavior, proceeding by the nucleation and propagation of a neck. Stoclet et al. analyzed the ductile regime in detail using in situ SAXS experiments [26]. PLLA showed the presence of shear bands and shear-band nucleated crazes during deformation in the linear domain. Upon further elongation, those shear-band nucleated crazes (at 45° to the load direction) intersected and nucleated standard crazes (perpendicular to the load direction). In the ductile deformation region after necking, the preferred plastic deformation mechanism of PLLA was standard crazing. The shear banding mechanism is generally observed for polymers with a high entanglement density, whereas crazing is observed for polymers with a low entanglement density. The entanglement length of PLLA ($M_e = 4{,}000$; Table 3) was intermediate between PS (main deformation mechanism crazing, $M_e = 19{,}100$ [29]) and PC (main deformation mechanism shear banding, $M_e = 2{,}490$ [29]), which might explain its mixed plastic deformation mechanism [26].

Stoclet et al. [26] suggested furthermore that the presence of voids at low deformation could be linked to the high aging rate of PLLA. Indeed, unaged PLLA was very ductile (Fig. 8) [30, 31], but it rapidly evolved towards brittle behavior.

Physical aging yields rearrangement of macromolecules to a denser and more ordered structure with a denser chain packing. The lost free volume and chain flexibility brings about higher yield stress and lower ductility [30].

In the brittle regime, which corresponds to the majority of use situations for PLLA, the crazes are nucleated before the yield point. At high crosshead speeds (as in the work of Stoclet et al. [26]) or low temperatures, failure generally occurs before yielding because the yield stress is higher than the critical stress for fibril break down [26]. The crazes turn then into cracks before the yield peak is reached.

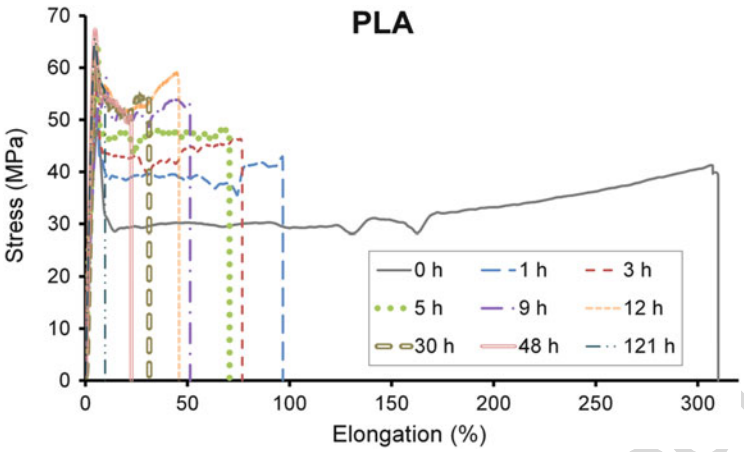

Fig. 8 Stress–strain (elongation) *curves* for amorphous PLLA at different aging times (23°C, 5 mm/min). From Ruellan et al. [31], personal communication

At lower crosshead speeds, such as 5 mm/min, yielding can be observed [27, 32, 33] with a yield stress typically around 50 MPa.

Table 5 shows a collection of typical data on the tensile properties of PLLA compared with other polymers. PLLA typically has an elongation at break of 5% and a yield strength of 60 MPa. Its features are similar to those of polystyrene (PS), but lower than those of polyethylene terephthalate (PET). The polyolefins show a lower stress at yield than PLLA but the strain at break of low-density polyethylene (LDPE) and high-density polyethylene (HDPE) are higher than that of PLLA. Compared with another biobased polymer, poly(hydroxybutyrate) (PHB), PLLA shows better mechanical properties with higher modulus of elasticity and stress at yield (Table 5).

No impact of the percentage of D-lactic acid in the macromolecular chain could be observed (Table 5). The molecular weight had moderate influence on the tensile properties, when analyzed in the frame of a single sample set (Table 5, sample set [34]). The crystallization of neat PLLA increased brittleness, which can be observed in sample sets from different studies [27, 33–35]. Annealing at different temperatures was reported to have an effect on the tensile properties. Samples crystallized at 110°C had higher tensile strength but lower elongation at break compared with amorphous samples, whereas annealing at 150°C caused lowering of both characteristics [35]. Cocca et al. also showed the importance of the crystal polymorph of PLLA on the mechanical properties. PLLA crystallized in the α-polymorph had higher Young's modulus and lower strain at break than PLLA crystallized in the α′-polymorph [36].

t5.1 **Table 5** Tensile testing properties of PLLA

t5.2 PLLA (% D)	χ_c (%)	M_w (kg/mol)	σ_y (MPa)	ε (%)	E (MPa)	Reference
t5.3 0	<10	23	59	1.5	3,550	[34]
t5.4 0	<10	66	59	7.0	3,750	[34]
t5.5 0	70	20	47	1.3	4,100	[34]
t5.6 0	45	66	66	4.0	4,150	[34]
t5.7 0	SC		50	5	3,500	[37][a]
t5.8 2	SC		60	6	3,500	[38][b]
t5.9 4.1	0	166	47	5		[27]
t5.10 4	SC		45	5	3,500	[37][c]
t5.11 4	0	182	57	4		[39]
t5.12 4.5	SC		60	6	3,500	[38][d]
t5.13 6.2	34	108	46	8		[40]
t5.14 8	0	223	47	8		[41]
t5.15 8	0	103	41	5		[33]
t5.16 8	43	122	53	5		[33]
t5.17 10	0	209	56	4.3		[39]
t5.18 10	0	242	64	6		[42]
t5.19 PET			69–172	60–165	2,206–4,275	[43]
t5.20 PS			46	1–2	2,890	[43]
t5.21 HDPE			19–24.5–30	10–586–1,000	800–950–1,400	[43]
t5.22 LDPE			9.6–10.3–25	270–620–706	165.5–248	[43, 44]
t5.23 PP[e]			25–35.5–44	20–37–800	1,300–1,380	[43, 44]
t5.24 PHB			31	7	910	[45]

t5.25 χ_c crystallinity degree, M_w molecular weight average, σ_y yield stress, ε elongation at break, E Young's modulus, *SC* semicrystalline; the exact crystallinity is not specified by the source

[a]Purapol L130, Corbion

[b]Ingeo 4032D, Natureworks

[c]Purapol LX175, Corbion

[d]Ingeo2003D, Natureworks

[e]Depends on specimen molding, history, and temperature of processing

404 *3.3 Toughening PLLA*

405 Improving the toughness of PLLA for increasing its applicative domains is a very
406 active research field. Roughly, four different techniques are employed: (1) biaxial
407 stretching, (2) external plasticizing with plasticizers, (3) blending with other poly-
408 mers, and (4) internal plasticizing by reactive extrusion.

409 Biaxial stretching is a processing method that allows the orientation of polymer
410 films, leading to an important change in the microstructure. A number of processes
411 result in de facto bi-oriented structures, such as film blowing, cable drawing, and
412 cast film bi-orientation. Bi-oriented PLLA is today commercially available for

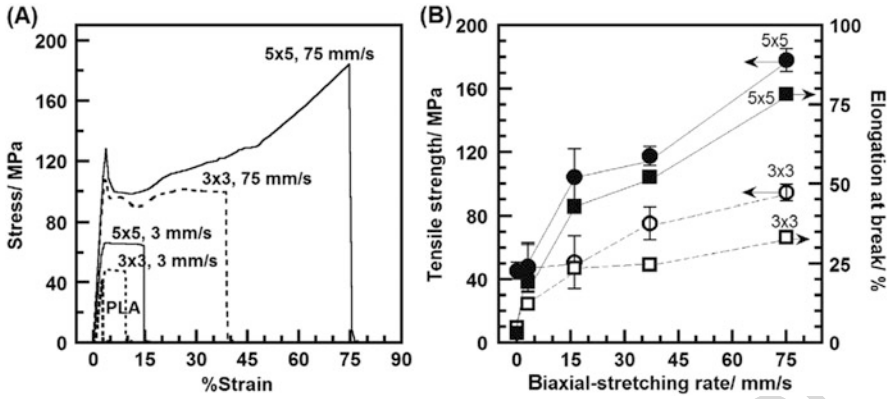

Fig. 9 Stress–strain *curves* (**a**) and tensile mechanical properties (**b**) of bi-oriented (90°C and preheating) PLLA (6% D, M_w 166 kg/mol). Reproduced with permission from Jariyasakoolroj et al. [52], Polymer, Elsevier

food packaging and other applications with an announced toughness of up to 180% elongation at break in the machine direction and 100% in the transverse direction (NatureWorks webpage [38]). The biaxial stretching of PLLA has been investigated by several authors [46–52], demonstrating the orientation of strain-induced or pre-existing crystallites in plane using either simultaneous or sequential stretching techniques. High stretching ratios (5 × 5) and stretching rates (75 mm/s) were favorable for a high toughness of PLLA (Fig. 9), because of the isotropic orientation of very small crystalline lamellae (α'-form), which developed from the irregular amorphous phase over the mesomorphic phase [52].

The influence of plasticizers on the mechanical properties of PLLA has been extensively studied and recently reviewed [53, 54]. Numerous external monomeric and oligomeric plasticizers were tested, the most prominent of which were poly(ethylene glycol) (PEG) [27, 41, 55–61] of variable molecular mass and citrate derivatives such as acetyl tributyl citrate (ATBC) [41, 59, 61–65]. Significant modifications of the mechanical properties were generally obtained at a plasticizer content of approximately 20 wt%, where T_g of the formulated materials was close to the tensile testing temperature. For example, at 20 wt% ATBC content in PLLA, the material presented a stress at break between 23.1 and 30 MPa and a strain at break above 298% [59, 61, 63, 65]. To preserve claims on biodegradability and biobased carbon content in plasticized PLLA, biobased and biodegradable molecules were extensively screened as plasticizers [53]. Epoxidized soybean oil [66–69] or epoxidized palm oil [69–71] were tested with some success. More recently, it was shown that the use of deodorizer distillates, which are a by-product of the vegetable oil industry, improved astonishingly the ductility of PLLA. The strain at break could be increased up to 130%, while the T_g of the formulated material remained higher than room temperature (45°C) and the yield strength at 24 MPa [39, 42]. Annealing of plasticized PLLA generally has a negative effect on toughness [33, 39, 40]. Piorkowska et al. [40] studied the mechanism involved and proposed that growing

crystalline lamellae expelled the plasticizer into the surrounding amorphous matrix. If plasticizer diffusion in the amorphous phase is not quick enough, this can lead to accumulation of the plasticizer next to the crystalline lamellae and, thus, weakening of the interface between the amorphous and crystalline phases, causing premature failure. The same authors also showed that, in some cases, phase separation between plasticizer and PLLA matrix can be positive for the mechanical properties of annealed samples, because the phase-separated plasticizer nodules can facilitate plastic deformation.

To toughen PLLA by melt blending, the most popular additions are biodegradable polyesters, mainly poly(caprolactone) (PCL), poly(butylene succinate) (PBS), and different members of the poly(hydroxyalkanoate) (PHA) family [54, 72]. For example, the inclusion of 10% PBS in PLLA caused an increase in the elongation at break of up to 120%. The impact of blend structure on the tensile properties was studied by Boufarguine et al. [73] with the help of the layer-multiplying co-extrusion process. This process consists of division of the extrusion flow and its reassembly in specially designed mixing elements, leading to multiplication of the number of co-extruded polymer layers. The increase in the number of PLLA and poly(hydroxybutyrate valerate) PBHV layers (in total 129 layers) allowed an elongation at break of 70%, which was more than the double the value obtained using a dry blend methodology (30%). The dry blend methodology consists of the mixing of polymer pellets offline and feeding them together into the extruder. Many alternative blending strategies exist for improving toughness, such as use of aliphatic-aromatic copolymers [e.g., poly(butylene adipate-*co*-terephthalate), PBAT], commercial acrylates, natural and synthetic rubbers, and impact modifiers [54]. Reactive extrusion processes were also recently reviewed [54, 74]. Reactive melt blending often relies on the reactivity of isocyanates reacting with the hydroxyl and carboxyl groups of PLLA and thereby improving compatibility of the two polymers. However, other functional chemical groups have also been used. Reactive grafting of citrates by maleic anhydride functionalized PLLA allowed an increase in strain at break comparable to that of externally plasticized PLLA, but without exudation of the plasticizer, even after 6 months of aging [75].

Blending of PLLA with a number of additives is also a possibility for improving the impact strength. Table 6 gives an overview of different results concerning this property, which is of interest for thermoformed containers and durable applications such as automotive parts. The impact strength of pristine PLLA (13 J/m) is low compared with that of other polymers, although the tensile modulus of PLLA is high (see Table 6). For example, the notched Izod impact strength of PS is 27 J/m and that of PET 56 J/m (data taken from [54]). The low impact strength is generally caused by low chain mobility in the polymer, which results in insufficient energy absorption and dissipation. The impact energy leads therefore to rapid failure propagation by breaking intermolecular bonds (from [76]). Annealing could increase the impact strength of pristine PLLA [34], but could have a negative effect on formulated samples [77]. Plasticizing, polymer blending, and the use of impact modifiers were tested with the aim of increasing impact strength. A number of commercial impact modifiers have been developed for PLLA. They are generally low-T_g elastomers or core–shell polymers. Core–shell polymers typically consist of

Table 6 Notched Izod impact strength (IS) of different PLLA formulations t6.1

	Notched Izod IS (kJ/m^2)	Reference	
PLLA	2.6	[54]	t6.3
Plasticizers			t6.4
PLLA/20% COPO1[a]	1.6	[81]	t6.5
PLLA/20% COPO2[a]	8.3	[81]	t6.6
PLLA/20% COPO3[a]	1.9	[81]	t6.7
PLLA/20% COPO4[a]	1.9	[81]	t6.8
Polymer blends			t6.9
PLLA/20% PBS	3.7	[54]	t6.10
PLLA + 20% PBAT[b]	4.4	[54]	t6.11
PLLA	3	[77]	t6.12
PLLA/30% SEBS[b]	16	[77]	t6.13
PLLA/20% SEBS/10% EGMA[b]	92	[77]	t6.14
Core–shell impact modifiers			t6.15
PLLA	3.4	[79]	t6.16
PLLA + 17% ethylene acrylate copolymer[c]	24	[79]	t6.17
(PLLA + 17% ethylene acrylate copolymer[c]) + 30% PMMA	44	[79]	t6.18
PLLA	3.6	[76]	t6.19
PLLA + 20% ethylene acrylate copolymer[d]	28.9	[76]	t6.20

[a]*COPO1* PLA-*b*-PEG350, *COPO2* PLA-*b*-PEG750, *COPO3* PLA-*b*-PEG400-*b*-PLA, *COPO4* three-star-(PEG-*b*-PLA) t6.21
[b]*PBAT* poly(butylene adipate-*co*-terephthalate
[c]*SEBS* hydrogenated styrene-*b*-butadiene-*b*-styrene copolymer, *EGMA* ethylene-*co*-glycidyl methacrylate (compatibilizer PLA/SEBS)
[d]Biomax Strong, DuPont Company

a rubbery (low-T_g) core surrounded by a glassy shell with good interfacial adhesion with the PLLA matrix. The impact modifiers are dispersed as microdomains in PLLA. The microdomains are able to absorb and dissipate mechanical energy upon impact or to retard or stop initiation and propagation of cracks. The average size of microdomains of impact modifiers in PLLA ranged in most studies between 0.1 and 5 μm [54, 76, 78–80]. Table 6 gives a selection of some results from the review of Liu et al. [54] and others collected from recent literature. It represents data obtained using the different toughening techniques, that is, plasticizing, polymer blending, and use of commercial impact modifiers. The decrease in microdomain size was, in general, positive for impact strength [54]. Interfacial adhesion between the impact modifier and the PLLA matrix is key to a successful increase in impact strength. The use of a compatibilizer can significantly enhance the material's properties. An example can be found in the study of Hashima et al. [77]. In this study, the use of a compatibilizer helped to improve PLLA impact strength up to 92 kJ/m^2 (Table 6). The drawback of the use of impact modifiers is a decrease in the modulus and stiffness of PLLA. For example, the modulus of PLLA in Bouzouita's study diminished from 3.2 to 2.3 GPa [79]. In conclusion, as already pointed out by Liu et al. [54], increasing PLLA impact strength while maintaining high stiffness still

505 remains a challenge. Furthermore, the effects of parameters such as the crystallinity
506 degree and the stereochemistry of PLLA still need to be investigated.

507 *3.4 Conclusion*

508 The mechanical properties of PLLA are intermediate between those of PS and PET,
509 which makes PLLA suitable for applications such as rigid containers, cases and
510 housings, service ware, and toys. The principal mechanisms responsible for
511 mechanical failure of PLLA have been intensively investigated in recent years
512 and much knowledge is now established. PLLA presents brittle fracture at room
513 temperature (at around 5% strain), which can be explained by a mixed mechanism
514 of crazing and shear banding. At temperatures higher than T_g, PLLA shows
515 extensive yielding and strain hardening. To overcome the limitations of the brittle
516 fracture and low impact strength, a number of strategies for toughening PLLA have
517 already been tested, such as bi-orientation, external and reactive plasticizing, and
518 melt blending with other polymers or commercial additives for increased impact
519 strength. Although there are already successful toughened PLLA products obtained
520 by bi-orientation and formulation with plasticizers and impact modifiers, research
521 in the field is very active, seeking novel additives (preferentially biobased and/or
522 biodegradable) and using melt blending strategies and reactive extrusion.

523 4 Barrier Properties of PLLA

524 The sorption/diffusion model [82] describes the permeability to gas and vapors in
525 polymers. Permeability is influenced by different intrinsic factors of a given
526 polymer, such as the free volume fraction (FFV) of the polymer, T_g, cohesive
527 energy density (CED), degree of crystallinity, molecular orientation, and copoly-
528 merization. A schematic representation of the different structural length scales that
529 are important for the transport of permeants in dense materials is shown in Fig. 10.
530 At the macroscopic length scale (Fig. 10a), the design of the global material
531 architecture (blend structures, multilayers, etc.) influences the barrier properties.
532 In particular, multilayer structures allow the barrier properties of two different
533 polymers to be combined. The permeability (P) of the material in that case is
534 roughly given by the following relationship:

$$\frac{1}{P} = \frac{w_1}{P_1} + \frac{w_2}{P_2}, \tag{4}$$

535 where w_1 and w_2 are the weight fractions of both polymers in the materials and
536 P_1 and P_2 their respective permeabilities. At smaller length scales (Fig. 10b), the
537 presence and morphology of impermeable obstacles in the pathway of diffusion
538 changes the transport properties. Those obstacles create a more tortuous and longer

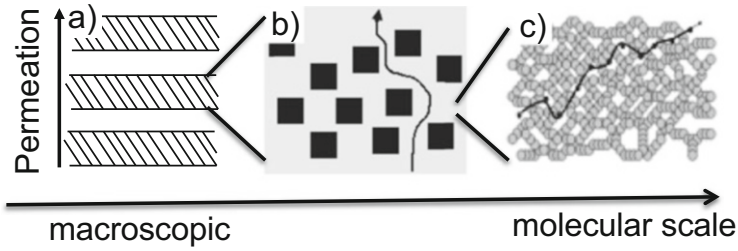

Fig. 10 Different length scales relevant for barrier properties: (**a**) macroscopic length scale of the material architecture (multilayer, blend, etc), (**b**) microscopic to nanoscopic length scale relevant for the tortuosity of the diffusive pathway circumventing obstacles (crystallites, fillers), and (**c**) macromolecular length scale of the hopping of permeants from one free volume void to another in the amorphous phase

pathway for the diffusive transport of solutes and, as a result, decrease the macroscopic diffusion coefficient. On the molecular scale (Fig. 10c), diffusion proceeds by successive hops of the permeant from one void in the polymer matrix to another. At high temperatures (above T_g), voids are redistributed rapidly and the diffusion rate is governed by the creation of voids of sufficient size for the permeant. In glassy polymers, the probability of the formation of voids of sufficient size is much smaller. The permeants therefore spend most of the time in one void, and only rarely local density fluctuations cause the opening of a tunnel which allows hopping of permeants from one void to the other. The overall diffusive transport is much slower than in melts or rubbers, but higher than extrapolation from the rubber state would predict because of the excess free volume in glasses [83–85].

PLLA barrier properties need to be improved for most applications, and in particular for food packaging [86–88]. Therefore, strategies for improvement using all the above-mentioned length scales have already been employed. The multilayer approach can achieve a broad range of properties that are not available for any of the individual materials/layers alone. Multilayer films can be prepared by co-extrusion, film lamination, or using a layer-by-layer approach. Co-extrusion consists of the simultaneous extrusion of two or more polymer layers and their assembly in the molten state. By contrast, film lamination is the combination of two or more films using an adhesive. The increase in tortuousity of the diffusive pathway inside PLLA has been pursued using two different approaches: (1) increasing polymer crystallinity, because the crystallites are impermeable to small molecules, and (2) adding fillers or nanofillers to the material [89]. The filler materials tested include clay and silicate nanoplatelets, silica nanoparticles (SiO_2), carbon nanotubes, graphene, cellulose-based nanofibers or nanowhiskers, and other inorganics.

4.1 Gas Barrier Properties

Oxygen has high applicative importance and, not surprisingly, most literature studies on gas barrier properties are concerned with the oxygen permeability, $P(O_2)$, of PLLA. Table 7 summarizes some experimental data on the oxygen permeability of PLLA compared with petrochemical polymers. PLLA performance is similar to that of PS and below the performance of PET.

$P(O_2)$ values between 1.3 and 2.0 $\times$ 10^{-18} m^3 m/m^2 s Pa at 30°C for amorphous PLLA have been reported, depending on the L/D ratio [90–92]. The oxygen transport coefficients of PLLA, whatever the L/D ratio, are sensitive to the measurement temperature and relative humidity (RH). Auras et al. [46] showed that at 0% RH, the oxygen permeability and solubility coefficients increased with temperature. Mensitieri et al. [93] investigated the coupled effects of water vapor and $P(O_2)$ and showed that PLLA, like other biopolymers, had lower oxygen barrier performance than petrochemical polymers, and that its performance was negatively influenced by its moisture susceptibility. The addition of plasticizers for the improvement of mechanical properties led to an increase in $P(O_2)$ as a result of higher mobility of the polymer chain and higher free volume brought by the plasticizer to the polymer matrix [33, 94]. In some cases, low molecular weight molecules can also fill in free volume, in which case they are positive for the

Table 7 Oxygen permeability of petrochemical polymers and biopolyesters [90–92, 96, 97]

Polymer	$P(O_2)$ $\times$ 10^{20} at 23°C and 50% or 0% RH (m^3 m/m^2 s Pa)
PLLA	130–300
Poly(3-hydroxy butyrate valerate) (PHBV)	50–157 (0% RH)
Polycaprolactone (PCL)	430 (0% RH)
Low-density polyethylene (LDPE)	2,200
High-density polyethylene (HDPE)	300
Polypropylene (PP)	550–1,100
Polystyrene (PS)	2,000
Polycarbonate (PC)	1,050
Poly(vinyl acetate) (PVA)	310
Poly(vinyl chloride) (PVC)	30
Poly(ethylene terephthalate) (PET)	10–60
Poly(ethylene naphthalate) (PEN)	5.7
Cellophane	1.6
Polyamide 6 (PA6)	1–30
Polyamide MXD6 (PA MXD6)	0.6
Liquid crystal polymer (LCP)	0.3
Poly(acrylonitrile) (PAN)	0.15–5
Poly(vinyl alcohol) (PVOH)	0.2–6.65 (0% RH)
Poly(vinylidene chloride) (PVDC)	0.1–3
Ethylene vinyl alcohol (EVOH)	0.002–1 (0% RH)

barrier properties. This was demonstrated by the use of low molecular weight lactic acid oligomers. The blending of PLLA with 25 wt% of lactic acid oligomers reduced the $P(O_2)$ by 22% [95].

Tailoring of the PLLA microstructure for an increase in its barrier properties has been widely investigated in recent years [91, 92, 98]. Dong et al. [99] reported a small increase in the oxygen barrier properties of bi-axially stretched and annealed PLLA. The initial $P(O_2)$ was 2.03×10^{-18} m^3 m/m^2 s Pa. After drawing with a stretching ratio of 3.5, the $P(O_2)$ decreased to 1.53×10^{-18} m^3 m/m^2 s Pa. In the case of stretched and annealed samples, the $P(O_2)$ decreased from 1.83×10^{-18} (stretching ratio 1 and annealed) to 1.31×10^{-18} m^3 m/m^2 s Pa (stretching ratio 3.5 and annealed) [99].

The effect of crystallinity on PLLA oxygen barrier properties was studied by several authors [33, 100–103]. However, there were a number of conflicting results, for which no clear relationship between PLLA crystallinity degree and barrier properties could be shaped. This situation was encountered in the case of several glassy polymers, as shown by Kanehasi et al. [104]. Guinault et al. [102] carried out a systematic study of the PLLA barrier properties as a function of the crystallinity degree. Their main results are shown in Fig. 11. The $P(O_2)$ of PLLA was either stable or even increased with increasing crystallinity degree (Fig. 11). Guinault et al. [102] showed that, in the case of crystallization of PLLA in α′-form crystallites, high percentages of dedensified rigid amorphous fraction were created in the amorphous phase. This produced a pathway of accelerated gas transport around the crystalline lamellae. The oxygen permeability coefficient of PLLA containing α-form crystallites was lower than that of PLLA containing α′-form crystallites [101],

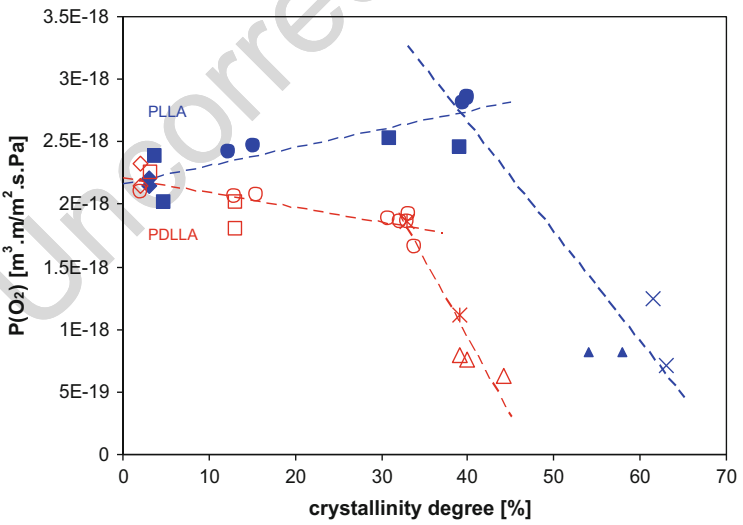

Fig. 11 Impact of thermal crystallization on the oxygen permeability of PLLA with two different % D (PLLA 1% D, PDLLA 4.3% D). Reproduced with permission from Guinault et al. [102], European Polymer Journal, Elsevier

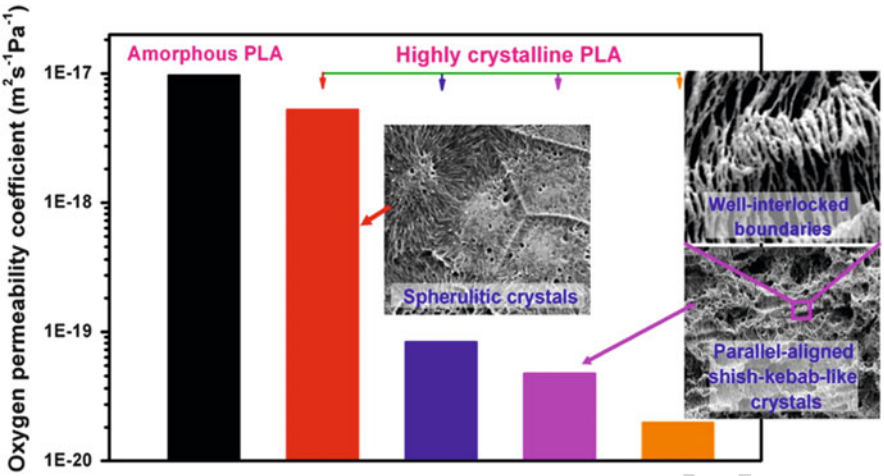

Fig. 12 Improvement in PLLA oxygen barrier properties by the formation of shish-kebab-like crystals. Reprinted with permission from Bai et al. [105], Biomacromolecules. Copyright 2016 American Chemical Society

because crystallization from the melt produced less dedensified amorphous phase [102]. To increase the gas barrier properties of PLLA, high tortuosity needs to be achieved and the formation of dedensified amorphous phases should be avoided.

Bai et al. [105] studied the $P(O_2)$ of PLLA with an original crystalline morphology, described as parallel-aligned shish-kebab-like crystals, with the aid of *N*,*N*′, *N*″-tricyclohexyl-1,3,5-benzene-tricarboxylamide (trade name TMC-328), a highly active nucleating agent. As shown in Fig. 12, the oxygen barrier performance of PLLA with such parallel-aligned shish-kebab-like crystals was more than two orders of magnitude higher than that of PLLA with spherulitic crystals. The growing crystalline lamellae interlocked at the boundary regions and thereby formed a very densely packed structure, which decreased the gas permeability. An increase in the concentration of nucleating agent from 0.2 to 0.5 wt% impacted the oxygen permeability. The PLLA with 0.5 wt% TMC sheet had a $P(O_2)$ of 1.989×10^{-20} m^3 m/m^2 s Pa, about 500 times lower than that of the amorphous PLLA sheets (9.692×10^{-18} m^3 m/m^2 s Pa) [105].

The second option for improving PLLA barrier properties, which has been widely studied, is an increase in tortuosity of the permeant pathway by the incorporation of inert, nanoscale fillers into PLLA [106–110]. The nanoscale particles need to have at least one dimension that is smaller than 100 nm, which yields a high aspect ratio (length/diameter = 100–500). The most widely used nanofillers are montmorillonites (MMTs). MMTs are hydrated alumina-silicate layered clays with a high surface area and large aspect ratio (50–1,000). Exfoliation of clay minerals in the polymer is of high importance for obtaining the desired high aspect ratio and a positive impact on the barrier properties. Furthermore, at a constant clay content, the permeability coefficient was reported to decrease as the length of the clay

particles increased [107, 111]. Using nanoclays such as organomodified MMT, Cloisite 25A (quaternary ammonium salt modified MMT), Cloisite 30B (alkyl quaternary ammonium salt bentonite), and organo-modified synthetic fluorine mica the permeability coefficient was globally divided by a factor of 2 or 3, depending on the type of nanoclay and the efficiency of exfoliation [112–114].

Guo et al [115] studied the $P(O_2)$ of PLLA and different nanocomposites using MMT, organomodified MMT, halloysite nanotubes, and organomodified halloysite nanotubes. They showed that the largest decrease in $P(O_2)$ was obtained using organomodified MMT. The halloysite nanotubes had no impact on the $P(O_2)$ of PLLA [115]. Picard et al. [107] reported a decrease in $P(O_2)$ of annealed crystalline films containing 4 wt% of MMT with respect to the amorphous reference PLLA film. They showed that the organomodified clays had a tortuosity effect in the matrix. A more important role of the nanofillers, however, was their effect as nucleating agents, which helped to achieve a high crystallinity degree for PLLA and thereby to decrease the $P(O_2)$ [107]. PLLA blended with 1 wt% of surface-modified nanoparticles by in situ polymerization of L-lactide using two different nanoparticles (nanosilica and Cloisite R 15A, an organomodified MMT) showed an increase both in crystallinity (up to 70%) and in barrier properties [116]. $P(O_2)$ was reduced by 80% and carbon dioxide and water vapor permeabilities were reduced by 50 and 45%, respectively, in comparison with pure PLLA [116].

Graphene and graphene oxide have been recently investigated as inorganic nanofillers for PLLA. To achieve a good dispersion of these nanofillers, Ambrosio-Martin tested pre-incorporation of graphene sheets by in situ melt polycondensation with lactic acid oligomers [117]. This procedure enhanced the barrier properties. Reductions of up to 45 and 41% in oxygen and water permeabilities, respectively, were reported. Graphene oxide is similar to graphene but the presence of some oxide groups allows better compatibility with the polar polymer matrix. Pinto et al. [118] reported that $P(O_2)$ decreased from 3.76×10^{-18} for pristine PLLA to $1.34–1.49 \times 10^{-18}$ m^3 m/m^2 s Pa for PLLA containing 0.2–0.6 wt% of graphene oxide. These authors obtained the same results for PLLA loaded with 0.2–0.6 wt% of graphene nanoplatelets.

In the framework of biobased and biodegradable materials, the increase in PLLA barrier properties was also attempted using organic and biobased materials. Tripathi and Katiyar [119] studied biocomposites obtained using microspheres composed of arabic gum grafted with lactic acid (LA-*g*-GA). A decrease in $P(O_2)$ by a factor of 10 was achieved independently of the amount of LA-*g*-GA (3, 5, 8, and 10%). Bionanocomposites of PLLA were also developed using cellulose nanostructures. Cellulose microfibrils (MFCs) have nanosized diameters (2–20 nm depending on the origin) and lengths in the micrometer range. The crystalline parts of MFCs can be isolated by several mechanical and chemical treatments, with the aim of obtaining cellulose nanocrystals (CNCs) or nanowhiskers. The lengths of CNC nanostructures range from 200 nm up to 1–2 μm and about 8–50 nm or less in diameter, which results in high aspect ratios [120–123]. Sanchez-Garcia et al. [124, 125] compared the effect of the same content of MFCs and CNCs. The addition of 5 wt% of MFCs had no effect on the gas barrier properties of PLLA

bionanocomposites whereas 5 wt% of CNCs slightly decreased (factor 2) the $P(O_2)$. This result was also shown by Espino et al. [121].

Furthermore, different strategies for the fabrication of multilayer materials with improved barrier properties were investigated. A bilayer sample composed of filtered 2,2,6,6-tetramethylpiperidine-1-oxyl (TEMPO)-radical oxidized cellulose nanofibers and PLLA was studied by Fukuzumi et al. [126] . Under dry conditions, the $P(O_2)$ of the multilayer system decreased by two orders of magnitude compared with neat PLLA. Martucci and Ruseckaite [127] proposed three-layer sheets based on glycerol-plasticized gelatin as the inner layer and PLLA as the outer layers. A decrease of $P(O_2)$ from 1.24×10^{-18} for neat PLLA to 0.81×10^{-18} m^3 m/m^2 s Pa for the three layers was reported. Svagan et al. [128] employed a layer-by-layer approach, using electrostatic forces to assemble alternating layers of MMT and chitosan on extruded PLLA film surfaces. When 70 MMT/chitosan bilayers were applied, the oxygen permeability was reduced by 99 and 96%, respectively, at 20 and 50% RH [128]. Novel processing techniques, such as layer-by-layer fabrication or layer-multiplying co-extrusion, permit the fabrication of materials with large numbers of layers having nanometer thickness (often between 20 and 100 nm). In these cases, the interface area in the multilayer material is very large and interface effects or interdiffusion of polymers at the interface have an effect on the material properties. Liu et al. [129] showed the potential of such materials to improve barrier properties. Boufarguine et al. [73] produced PLLA-PHBV multilayer films (129 layers) by layer-multiplying co-extrusion. They showed that the multiplication of the layer number had a positive effect on the helium permeability, compared with the three-layer PLLA-PHBV-PLLA configuration. The helium permeability decreased from 120×10^{-18} to 77.6×10^{-18} and 74.3×10^{-18} m^3 m/m^2 s Pa for materials having 129 and 3 layers, respectively.

The carbon dioxide permeability coefficient of PLLA is 2.5×10^{-18} m^3 m/m^2 s Pa, which is lower than that of LDPE and PS (95 and 17 m^3 m/m^2 s Pa, respectively) [92]. PET is a better barrier against CO_2 as its permeability coefficient is as low as 0.5 m^3 m/m^2 s Pa. The CO_2 permeability was shown to increase with L-lactic acid content and temperature [46]. The crystallization of PLLA induced a decrease in the carbon dioxide permeability coefficient [130, 131]. According to Sawada et al. [103], the decrease in CO_2 permeability with an increase in crystallinity can only be achieved at a crystallinity degree higher than 40%.

The nitrogen permeability of PLLA is 3.8×10^{-19} m^3 m/m^2 s Pa, which is lower than the values for PS (5.9×10^{-19} m^3 m/m^2 s Pa) and LDPE (73×10^{-19} m^3 m/m^2 s Pa) at 25°C but higher than that of unplasticized PVC (0.88×10^{-19} m^3 m/m^2 s Pa) [92]. The L/D ratio did not affect the nitrogen permeability of PLLA [132]. The crystallinity effect has also been evaluated for this gas and it seems that the nitrogen permeability decreased with the increase in crystallinity degree of PLLA [103].

The gas selectivity of PLLA membranes depends on the chosen gas. Lehermeier et al. [133] showed that the separation factor of CH_4 and CO_2, equal to 10, was not dependent on the crystallinity or L/D ratio. Only a change in temperature made it possible to increase this factor. Sawada et al. [103] confirmed the inefficiency of crystallinity on the permselectivity, but also showed that the diffusivity and solubility selectivity were not influenced by the crystallinity. The gas permselectivity in

PLLA is larger than 120 for H_2/N_2, 6 for O_2/N_2, 23 for CO_2/N_2, 27 for CO_2/CH_4, and 1 for CH_4/N_2 [103]. The permselectivity of PLLA is twice that of LDPE and PVC for O_2/N_2 and CO_2/N_2 [134]. The solubility coefficients of O_2, N_2, CO_2, and CH_4 decreased monotonically with increasing crystallization temperature: PLLA-70 > PLLA-80 > PLLA-90 > PLLA-150 [135].

4.2 *Water Vapor Permeability of PLLA*

Table 8 summarizes the water vapor transmission rate (WVTR) of PLLA compared with other commodity polymers. The WVTR is a water vapor permeability measure widely used in academic and industrial literature. Table 9 also gives the permeability values in international standard units. PLLA has the highest water vapor permeability, $P(H_2O)$, of the polyesters. To promote PLLA as a biobased packaging for aqueous food products, an improvement in the water vapor barrier must be achieved. The design target is to close the gap between the $P(H_2O)$s of PLLA and PET.

Table 8 Comparison of water vapor transmission rates for PLLA and other polymers, compiled from [46, 50, 125, 137, 139, 143]

Polymer	Water vapor transmission rate at 23°C and 85% RH (g mm/m^2 day)
PLLA	1.8–2.3
Low density polyethylene (LDPE)	0.2–0.6
High density polyethylene (HDPE)	0.04–0.16
Polypropylene (PP)	0.2–0.4
Polystyrene (PS)	1–10
Polycarbonate (PC)	9–15
Poly(ethylene terephthalate) (PET)	0.5–2
Poly(ethylene naphthalate) (PEN)	0.7
Cellophane	165
Polyamide 6 (PA6)	0.3–10
Polyamide MXD6 (PA MXD6)	0.6
Liquid crystal polymer (LCP)	0.03
Poly(acrylonitrile) (PAN)	1–10
Poly(vinyl alcohol) (PVOH)	0.1
Poly(vinylidene chloride) (PVDC)	0.05–0.12
Ethylene vinyl alcohol (EVOH)	1–3

t9.1 **Table 9** Water vapor permeability of different polymers

t9.2	Polymer	$P(H_2O) \times 10^{-13}$ (kg m/s m^2 Pa)	Reference
t9.3	PLLA	0.109–0.126	[96, 97, 121, 123]
t9.4	PHBV	0.012–0.069	[96, 97]
t9.5	PCL	0.091	[96, 97]
t9.6	PET	0.03	[96, 97]

There are some contradictory results in the literature on the effect of temperature and RH on the $P(H_2O)$ of PLLA. Auras et al. [46] showed a decrease in permeability with increasing temperature whereas Shogren reported an increase [136]. Siparsky et al. [137] showed that the diffusion coefficients increased and the solubility coefficients decreased with the temperature at 90% RH, which was contradicted by Holm et al. who showed higher values of moisture sorption at higher temperatures [138]. Furthermore, the conclusions on the effect of the crystallinity degree on the barrier properties were different in different studies. In some works, a higher crystallinity degree caused a slight improvement in the barrier properties [69, 136, 139] and in others not [137]. These discrepancies in the data show that the mechanism of water transport in PLLA is still not completely understood [140]. In particular, the presence of water clusters in the PLLA matrix and their potential to diffuse in cluster form are still controversial [141]. Indeed, water can cluster inside the PLLA matrix, which changes the structure of the diffusing unit. Water diffusion in the form of clusters would reduce the rate of diffusion compared with the diffusion of single molecules. Davis et al. [142] described non-Fickian diffusion of water in PLLA. At small time intervals, water transport was driven by the diffusion coefficient, whereas with long experiment times non-Fickian diffusion occurred as a result of slow polymer relaxation and swelling by water sorption. The diffusion coefficients were shown to be constant with water activity and concentration and to increase with temperature.

The strategies used to improve $P(H_2O)$ were essentially the same as used for improving $P(O_2)$. Delpouve et al. [50] showed that biaxial stretching had a positive impact on $P(H_2O)$ in that it reduced the diffusion coefficient at high stretching ratios. However, if a thermal annealing treatment was added after biaxial stretching, the positive effect of the treatment on the barrier properties was lost. Similar to the case of oxygen barrier properties, thermal crystallization was not efficient enough to induce sufficient tortuosity in the permeant pathway. Slackening of the orientation in the amorphous phase after thermal annealing of the biaxially stretched samples could be one reason for the regression of barrier properties observed between oriented and annealed PLLA [144]. Cocca et al. reported that crystallization of PLLA in the α-polymorph was more efficient at increasing water barrier properties than α′-form crystallites [36]. Tsuji et al. [145] studied the crystalline structure and $P(H_2O)$ of poly(L-lactide)/poly(D-lactide) blend films. The results showed that the stereoregularity of the composite structure improved the water vapor barrier properties. Nanocomposites were also fabricated with the aim of decreasing $P(H_2O)$. For example, biodegradable PLLA/poly(trimethylene-

carbonate)/laponite (2 wt%) composite films achieved an improvement in $P(H_2O)$. The value of $P(H_2O)$ decreased from 4.57×10^{-13} to 3.23×10^{-13} kg m/m^2 s Pa [146]. A small improvement in $P(H_2O)$ was also obtained using chemically grafted cellulose nanocrystals as nanofillers in PLLA [123]. Deposition of alternate layers of chitosan and processed cellulose nanocrystals on PLLA films and bottles was studied by Halasz et al. [147]. Using the layer-by-layer (LbL) technique, PLLA was coated with four bilayers of chitosan and cellulose nanocrystals. An improvement in $P(H_2O)$ of 29 and 26% was obtained for PLLA films and bottles, respectively [147].

4.3 Permeability of Organic Vapors Through PLLA

The transport of organic compounds in PLLA has been the subject of only a few studies, although it is of importance in food packaging applications. Ethylene, a compound accelerating fresh food ripening, plays an important role in the storage of fresh fruits. The ethylene permeability of amorphous PLLA has been tested and evaluated to be 6.8×10^{-18} m^3 m/m^2 s Pa [133]. This value is higher than the ethylene permeability of PET (3.0×10^{-20} m^3 m/m^2 s Pa) [133] but lower than the value for LDPE (2.2×10^{-17} m^3 m/m^2 s Pa) [91]. Increasing the crystallinity of PLLA induced a decrease in ethylene permeability [103, 133].

The transport coefficients for ethyl acetate, an aroma booster found in a large variety of aroma formulations, were calculated from sorption of ethyl acetate in PLLA. The ethyl acetate permeability of PLLA was 5.34×10^{-19} kg m/m^2 s Pa at 30°C and 0.3 activity. This value was higher than that for PET but lower than those of PP and LDPE. However, the ethyl acetate solubility coefficient in PLLA, 6.17×10^{-3} kg m^{-3} Pa^{-1} at 30°C and 0.3 activity, was higher than that of the other polymers [148]. This result was comparable to the value reported by Colomines et al. [100] for an amorphous PLLA with 99% L-lactide content at 25°C and 0.5 activity. Moreover, increasing the crystallinity of PLLA provoked a decrease in the ethyl acetate solubility coefficient at 0.5 and 0.9 activity [33, 100]. The permeability of limonene through PLLA was estimated at a maximal value of 9.96×10^{-21} kg m/m^2 s Pa at 45°C and with a limonene partial pressure of 258 Pa. The permeability value of this more hydrophobic molecule is lower than that of ethyl acetate in PLLA and those measured for PET, PP, and LDPE [148, 149].

A study of scalping aroma compounds by PLLA during high-pressure treatment evidenced a lower uptake of organic molecules by PLLA compared with LDPE. Indeed, ethyl hexanoate and limonene were more sorbed in the more apolar matrix, LDPE. By contrast, the more polar molecules 2-hexanone and ethyl butanoate were more sorbed by the more polar polymer matrix PLLA [150–152].

The barrier properties of PLLA towards organic compounds depend on the diffusion and solubility coefficients of the given organic molecule. Colomines et al. [100] and Courgneau et al. [33] studied ethyl acetate sorption in PLLA at activities up to 0.5 in Colomines's paper and 0.2 in Courgneau's paper. At these

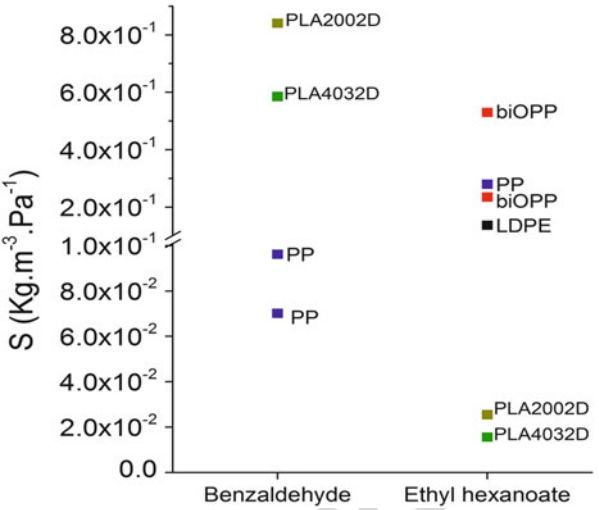

Fig. 13 Solubility coefficients of aroma compounds for different grades of PLLA compared with polyolefins. Data were taken from [151]

high activities, the sorption of ethyl acetate into PLLA induced morphological changes in the polymer structure, namely plasticization and induced crystallization. These changes could lead to several discrepancies in solubility coefficient data in the literature at various activities. Nevertheless, Auras et al [148], and Salazar et al. [152] demonstrated that, whatever the methodologies used, the solubility coefficients of ethyl acetate in PLLA were close to 6.17×10^{-3} kg m^{-3} Pa^{-1} at 30°C. These results showed that, at low activity, data could be compared and the solubility coefficient was independent of partial pressure following Henry's law. At low activity, the sorption of ethyl acetate in PLLA films is similar to that reported for PET, LDPE, and PP. In the case of ethyl hexanoate, its solubility coefficient in different grades of PLLA is ten times lower than in bi-axially oriented polypropylene (biOPP), PP, and LDPE (Fig. 13). Benzaldehyde presented a solubility coefficient in PLLA that was ten times higher than that in PP [152], which could lead to solvent-induced crystallization and plasticization and, thus, changes in PLLA barrier properties [152]. The high affinity of PLLA for molecules with aromatic functions can be explained by the miscibility of PLLA with aromatic solvents such as toluene and benzene [153, 154]. In mixture, the presence of benzaldehyde favors the interaction and sorption of other organic compounds in PLLA [152].

4.4 Nonvolatile Compounds

The barrier properties of PLLA against oil products have been rarely studied. Rapeseed oil and oil-in-water emulsions were packed in PLLA trays and stored for 30 days at 40°C. For emulsions with 40% oil content, sorption of oil was very low (<5 mg/dm^2 of material) whereas the sorption reached 10 mg/dm^2 of material

when PLLA was in contact with rapeseed oil. PET samples immersed in olive oil for 10 days at 40°C sorbed 33 mg/dm^2. These results, obtained with the same experimental procedure, indicate that PLLA could be an alternative candidate to PET for the conditioning of oil and fatty products [152].

4.5 Conclusion

Barrier properties are of importance for a number of applications, especially packaging. For the preservation of packed goods, low permeability to water, oxygen, and organic vapors is often required. However, these objectives are contradictory in that a high oxygen barrier can be reached by polar materials, whereas polar materials are not a barrier to water vapor. Therefore, numerous strategies have been used to create obstacles to permeation inside the polymer matrix. Crystallization of semicrystalline polymers can be efficient in this respect but, in the case of PLLA, thermal crystallization does not necessarily lead to improvements in barrier properties because of the formation of dedensified phases in the polymer matrix. Controlling crystallite morphology is very important and the most interesting increases in barrier properties could be obtained by shish-kebab-like structures. An alternative strategy is the fabrication of nanocomposites. Incorporation of nanofillers had two effects: (1) an increase in the tortuosity of the diffusive pathway of molecules and, more importantly, (2) an increase in PLLA crystallinity because of the nucleating effect. Strategies using multilayer materials were also efficient, and novel processing methods allowing the creation of multilayers with a large number of layers have shown promising results for the improvement of barrier properties in other polymers. In conclusion, improvement of PLLA barrier properties is still an active research topic and approaches for tailoring crystalline morphology and use of fillers or multilayers will be investigated.

References

1. Garlotta D (2001) A literature review of poly(lactic acid). J Polym Environ 9(2):63–84
2. Dorgan JR, Janzen J, Knauss DM, Hait SB, Limoges BR, Hutchinson MH (2005) Fundamental solution and single-chain properties of polylactides. J Polym Sci B Polym Phys 43(21):3100–3111. doi:10.1002/polb.20577
3. Chile L-E, Mehrkhodavandi P, Hatzikiriakos SG (2016) A comparison of the rheological and mechanical properties of isotactic, syndiotactic, and heterotactic poly(lactide). Macromolecules 49(3):909–919. doi:10.1021/acs.macromol.5b02568
4. Kim ES, Kim BC, Kim SH (2004) Structural effect of linear and star-shaped poly(L-lactic acid) on physical properties. J Polym Sci B Polym Phys 42(6):939–946. doi:10.1002/polb.10685
5. Othman N, Jazrawi B, Mehrkhodavandi P, Hatzikiriakos SG (2012) Wall slip and melt fracture of poly(lactides). Rheol Acta 51(4):357–369. doi:10.1007/s00397-011-0613-7

6. Othman N, Acosta-Ramirez A, Mehrkhodavandi P, Dorgan JR, Hatzikiriakos SG (2011) Solution and melt viscoelastic properties of controlled microstructure poly(lactide). J Rheol 55(5):987–1005. doi:10.1122/1.3609853
7. Palade LI, Lehermeier HJ, Dorgan JR (2001) Melt rheology of high L-content poly(lactic acid). Macromolecules 34(5):1384–1390. doi:10.1021/ma001173b
8. Van Krevelen DW, Te Nijenhuis K (2009) Properties of polymers, 4th edn. Elsevier, Amsterdam. doi:10.1016/B978-0-08-054819-7.00001-7
9. Dorgan JR, Williams JS, Lewis DN (1999) Melt rheology of poly(lactic acid): Entanglement and chain architecture effects. J Rheol 43(5):1141–1155. doi:10.1122/1.551041
10. Grijpma DW, Penning JP, Pennings AJ (1994) Chain entanglement, mechanical-properties and drawability of poly(lactide). Colloid Polym Sci 272(9):1068–1081. doi:10.1007/bf00652375
11. Dorgan JR, Janzen J, Clayton MP, Hait SB, Knauss DM (2005) Melt rheology of variable L-content poly(lactic acid). J Rheol 49(3):607–619. doi:10.1122/1.1896957
12. Blomqvist J (2001) RIS metropolis Monte Carlo studies of poly(L-lactic), poly(L,D-lactic) and polyglycolic acids. Polymer 42(8):3515–3521. doi:10.1016/s0032-3861(00)00704-7
13. Fang Q, Hanna MA (1999) Rheological properties of amorphous and semicrystalline polylactic acid polymers. Ind Crop Prod 10(1):47–53. doi:10.1016/s0926-6690(99)00009-6
14. Dean KM, Petinakis E, Meure S, Yu L, Chryss A (2012) Melt strength and rheological properties of biodegradable poly(lactic acid) modified via alkyl radical-based reactive extrusion processes. J Polym Environ 20(3):741–747. doi:10.1007/s10924-012-0461-2
15. Zhang JL, Li G, Su YZ, Qi RR, Ye DD, Yu J, Huang SW (2012) High-viscosity polylactide prepared by in situ reaction of carboxyl-ended polyester and solid epoxy. J Appl Polym Sci 123(5):2996–3006. doi:10.1002/app.34951
16. Dorgan JR, Lehermeier H, Mang M (2000) Thermal and rheological properties of commercial-grade poly(lactic acid)s. J Polym Environ 8(1):1–9. doi:10.1023/a:1010185910301
17. Al-Itry R, Lamnawar K, Maazouz A (2015) Biopolymer blends based on poly (lactic acid): shear and elongation rheology/structure/blowing process relationships. Polymers 7(5):939–962. doi:10.3390/polym7050939
18. Schneider J, Manjure S, Narayan R (2016) Reactive modification and compatibilization of poly(lactide) and poly(butylene adipate-co-terephthalate) blends with epoxy functionalized-poly(lactide) for blown film applications. J Appl Polym Sci 133(16):43310. doi:10.1002/app.43310
19. Wang LY, Jing XB, Cheng HB, Hu XL, Yang LX, Huang YB (2012) Rheology and crystallization of long-chain branched poly(L-lactide)s with controlled branch length. Ind Eng Chem Res 51(33):10731–10741. doi:10.1021/ie300524j
20. Ma PM, Shen TF, Xu PW, Dong WF, Lemstra PJ, Chen MQ (2015) Superior performance of fully biobased poly(lactide) via stereocomplexation-induced phase separation: structure versus property. ACS Sustain Chem Eng 3(7):1470–1478. doi:10.1021/acssuschemeng.5b00208
21. Zhang X, Schneider K, Liu G, Chen J, Brüning K, Wang D, Stamm M (2012) Deformation-mediated superstructures and cavitation of poly (L-lactide): in-situ small-angle X-ray scattering study. Polymer 53(2):648–656. doi:10.1016/j.polymer.2011.12.002
22. Pawlak A, Galeski A, Rozanski A (2014) Cavitation during deformation of semicrystalline polymers. Prog Polym Sci 39(5):921–958. doi:10.1016/j.progpolymsci.2013.10.007
23. Stoclet G, Seguela R, Lefebvre JM, Elkoun S, Vanmansart C (2010) Strain-induced molecular ordering in polylactide upon uniaxial stretching. Macromolecules 43(3):1488–1498. doi:10.1021/ma9024366
24. Mulligan J, Cakmak M (2005) Nonlinear mechanooptical behavior of uniaxially stretched poly(lactic acid): dynamic phase behavior. Macromolecules 38(6):2333–2344

25. Stoclet G, Seguela R, Lefebvre JM, Li S, Vert M (2011) Thermal and strain-induced chain ordering in lactic acid stereocopolymers: influence of the composition in stereomers. Macromolecules 44(12):4961–4969. doi:10.1021/ma200469t
26. Stoclet G, Lefebvre JM, Seguela R, Vanmansart C (2014) In-situ SAXS study of the plastic deformation behavior of polylactide upon cold-drawing. Polymer 55(7):1817–1828. doi:10.1016/j.polymer.2014.02.010
27. Kulinski Z, Piorkowska E (2005) Crystallization, structure and properties of plasticized poly (L-lactide). Polymer 46(23):10290–10300. doi:10.1016/j.polymer.2005.07.101
28. Galeski A (2003) Strength and toughness of crystalline polymer systems. Prog Polym Sci 28(12):1643–1699. doi:10.1016/j.progpolymsci.2003.09.003
29. Kramer EJ (1984) Craze fibril formation and breakdown. Polym Eng Sci 24(10):761–769. doi:10.1002/pen.760241006
30. Pan PJ, Zhu B, Inoue Y (2007) Enthalpy relaxation and embrittlement of poly(L-lactide) during physical aging. Macromolecules 40(26):9664–9671. doi:10.1021/ma071737c
31. Ruellan A (2015) Conception raisonée à l'aide de la formulation et du procédé d'un film souple biosourcé et biodégradable pour l'emballage alimentaire. Université Paris-Saclay–ParisTech, Maassy
32. Kulinski Z, Piorkowska E, Gadzinowska K, Stasiak M (2006) Plasticization of poly(l-lactide) with poly(propylene glycol). Biomacromolecules 7(7):2128–2135
33. Courgneau C, Domenek S, Lebosse R, Guinault A, Averous L, Ducruet V (2012) Effect of crystallization on barrier properties of formulated polylactide. Polym Int 61(2):180–189. doi:10.1002/pi.3167
34. Perego G, Cella GD, Bastioli C (1996) Effect of molecular weight and crystallinity on poly (lactic acid) mechanical properties. J Appl Polym Sci 59(1):37–43. doi:10.1002/(SICI)1097-4628(19960103)59:1<37::AID-APP6>3.0.CO;2-N
35. Renouf-Glauser AC, Rose J, Farrar DF, Cameron RE (2005) The effect of crystallinity on the deformation mechanism and bulk mechanical properties of PLLA. Biomaterials 26(29): 5771–5782. doi:10.1016/j.biomaterials.2005.03.002
36. Cocca M, Di Lorenzo ML, Malinconico M, Frezza V (2011) Influence of crystal polymorphism on mechanical and barrier properties of poly(L-lactic acid). Eur Polym J 47: 1073–1080
37. Corbion. PLA polymers. http://www.corbion.com/bioplastics/products/pla-polymers. Accessed 28 April 2016
38. NatureWorks (2016) Food and beverage packaging. http://www.natureworksllc.com/Product-and-Applications/Films
39. Ruellan A, Ducruet V, Gratia A, Saelices Jimenez L, Guinault A, Sollogoub C, Chollet G, Domenek S (2016) Palm oil deodorizer distillate as toughening agent in polylactide packaging films. Polym Int 65(6):683–690. doi:10.1002/pi.5114
40. Piorkowska E, Kulinski Z, Galeski A, Masirek R (2006) Plasticization of semi-cristalline poly(L-lactide) with poly(propylene glycol). Polymer 47(20):7178–7188
41. Courgneau C, Domenek S, Guinault A, Averous L, Ducruet V (2011) Analysis of the structure-properties relationships of different multiphase systems based on plasticized poly (lactic acid). J Polym Environ 19(2):362–371. doi:10.1007/s10924-011-0285-5
42. Ruellan A, Guinault A, Sollogoub C, Chollet G, Ait-Mada A, Ducruet V, Domenek S (2015) Industrial vegetable oil by-products increase the ductility of polylactide. Express Polym Lett 9(12):1087–1103. doi:10.3144/expresspolymlett.2015.98
43. Brandrup J, Immergut EH, Grulke EA (2003) Polymer handbook, 4th edn. Wiley-Interscience, Hoboken
44. Strapasson R, Amico SC, Pereira MFR, Sydenstricker THD (2005) Tensile and impact behavior of polypropylene/low density polyethylene blends. Polym Test 24(4):468–473. doi:10.1016/j.polymertesting.2005.01.001
45. Baltieri RC, Mei LHI, Bartoli J (2003) Study of the influence of plasticizers on the thermal and mechanical properties of poly(3-hydroxybutyrate) compounds. Macromol Symp 197: 33–44

46. Auras RA, Harte B, Selke S, Hernandez R (2003) Mechanical, physical, and barrier properties of poly(lactide) films. J Plast Film Sheet 19(2):123–135
47. Ou X, Cakmak M (2010) Comparative study on development of structural hierarchy in constrained annealed simultaneous and sequential biaxially stretched polylactic acid films. Polymer 51(3):783–792. doi:10.1016/j.polymer.2009.11.058
48. Smith PB, Leugers A, Kang SH, Hsu SL, Yang XZ (2001) An analysis of the correlation between structural anisotropy and dimensional stability for drawn poly(lactic acid) films. J Appl Polym Sci 82(10):2497–2505. doi:10.1002/app.2100
49. Tsai CC, Wu RJ, Cheng HY, Li SC, Siao YY, Kong DC, Jang GW (2010) Crystallinity and dimensional stability of biaxial oriented poly(lactic acid) films. Polym Degrad Stab 95(8): 1292–1298. doi:10.1016/j.polymdegradstab.2010.02.032
50. Delpouve N, Stoclet G, Saiter A, Dargent E, Marais S (2012) Water barrier properties in biaxially drawn poly(lactic acid) films. J Phys Chem B 116(15):4615–4625. doi:10.1021/jp211670g
51. Ou X, Cakmak M (2008) Influence of biaxial stretching mode on the crystalline texture in polylactic acid films. Polymer 49:5344–5352
52. Jariyasakoolroj P, Tashiro K, Wang H, Yamamoto H, Chinsirikul W, Kerddonfag N, Chirachanchai S (2015) Isotropically small crystalline lamellae induced by high biaxial-stretching rate as a key microstructure for super-tough polylactide film. Polymer 68:234–245. doi:10.1016/j.polymer.2015.05.006
53. Ruellan A, Ducruet V, Domenek S (2015) Plasticization of poly(lactide). In: Jiménez A, Peltzer M, Ruseckaite RA (eds) Poly(lactic acid) science and technology: processing, properties, additives and applications. The Royal Society of Chemistry, London, pp. 124–170. doi:10.1039/9781782624806-00124
54. Liu HZ, Zhang JW (2011) Research progress in toughening modification of poly(lactic acid). J Polym Sci B Polym Phys 49(15):1051–1083. doi:10.1002/polb.22283
55. Hu Y, Hu YS, Topolkaraev V, Hiltner A, Baer E (2003) Crystallization and phase separation in blends of high stereoregular poly(lactide) with poly(ethylene glycol). Polymer 44: 5681–5689
56. Sheth M, Kumar RA, Davé V, Gross RA, McCarthy SP (1997) Biodegradable polymer blends of poly(lactic acid) and poly(ethylene glycol). J Appl Polym Sci 66:1495–1505
57. Jacobsen S, Fritz HG (1999) Plasticizing polylactide—the effect of different plasticizers on the mechanical properties. Polym Eng Sci 39(7):1303–1310. doi:10.1002/pen.11517
58. Martin O, Averous L (2001) Poly(lactic acid): plasticization and properties of biodegradable multiphase systems. Polymer 42(14):6209–6219
59. Baiardo M, Frisoni G, Scandola M, Rimelen M, Lips D, Ruffieux K, Wintermantel E (2003) Thermal and mechanical properties of plasticized poly(L-lactic acid). J Appl Polym Sci 90(7):1731–1738. doi:10.1002/app.12549
60. Pillin I, Montrelay N, Grohens Y (2006) Thermo-mechanical characterization of plasticized PLA: is the miscibility the only significant factor? Polymer 47(13):4676–4682
61. Ruellan A, Guinault A, Sollogoub C, Ducruet V, Domenek S (2015) Solubility factors as screening tools of biodegradable toughening agents of polylactide. J Appl Polym Sci 132: 42476. doi:10.1002/APP.42476
62. Ljungberg N, Andersson T, Wesslén B (2003) Film extrusion and film weldability of poly (lactic acid) plasticized with triacetine and tributyl citrate. J Appl Polym Sci 88:3239–3247
63. Labrecque LV, Kumar RA, Davé V, Gross RA, McCarthy SP (1997) Citrate esters as plasticizers for poly(lactic acid). J Appl Polym Sci 66:1507–1513
64. Yu J, Wang N, Ma X (2008) Fabrication and characterization of poly(lactic acid)/acetyl tributyl citrate/carbon black as conductive polymer composites. Biomacromolecules 9(3): 1050–1057
65. Murariu M, Ferreira ADS, Alexandre M, Dubois P (2008) Polylactide (PLA) designed with desired end-use properties: 1. PLA compositions with low molecular weight ester-like plasticizers and related performances. Polym Adv Technol 19:636–646

66. Ali F, Chang Y-W, Kang SC, Yoon JY (2009) Thermal, mechanical and rheological properties of poly (lactic acid)/epoxidized soybean oil blends. Polym Bull 62(1):91–98. doi:10.1007/s00289-008-1012-9
67. Xu YQ, Qu JP (2009) Mechanical and rheological properties of epoxidized soybean oil plasticized poly(lactic acid). J Appl Polym Sci 112(6):3185–3191. doi:10.1002/app.29797
68. Xiong Z, Yang Y, Feng J, Zhang X, Zhang C, Tang Z, Zhu J (2012) Preparation and characterization of poly(lactic acid)/starch composites toughened with epoxidized soybean oil. Carbohydr Polym 92(1):810–816. doi:10.1016/j.carbpol.2012.09.007
69. Al-Mulla EAJ, Yunus W, Ibrahim NAB, Ab Rahman MZ (2010) Properties of epoxidized palm oil plasticized polytlactic acid. J Mater Sci 45(7):1942–1946. doi:10.1007/s10853-009-4185-1
70. Silverajah VSG, Ibrahim NA, Zainuddin N, Yunus W, Abu Hassan H (2012) Mechanical, thermal and morphological properties of poly(lactic acid)/epoxidized palm olein blend. Molecules 17(10):11729–11747. doi:10.3390/molecules171011729
71. Silverajah VSG, Ibrahim NA, Yunus W, Abu Hassan H, Woei CB (2012) A comparative study on the mechanical, thermal and morphological characterization of poly(lactic acid)/epoxidized palm oil blend. Int J Mol Sci 13(5):5878–5898. doi:10.3390/ijms13055878
72. Anderson KS, Schreck KM, Hillmyer MA (2008) Toughening polylactide. Polym Rev 48(1):85–108. doi:10.1080/15583720701834216
73. Boufarguine M, Guinault A, Miquelard-Garnier G, Sollogoub C (2013) PLA/PHBV films with improved mechanical and gas barrier properties. Macromol Mater Eng 298(10):1065–1073. doi:10.1002/mame.201200285
74. Raquez JM, Ramy-Ratiarison R, Murariu M, Dubois P (2015) Reactive extrustion of PLA-based materials: from synthesis to reactive melt-blending. In: Poly(lactic acid) science and technology: processing, properties, additives and applications. The Royal Society of Chemistry, London, pp. 101–123. doi:10.1039/9781782624806-00124
75. Hassouna F, Raquez J-M, Addiego F, Toniazzo V, Dubois P, Ruch D (2012) New development on plasticized poly(lactide): chemical grafting of citrate on PLA by reactive extrusion. Eur Polym J 48(2):404–415. doi:10.1016/j.eurpolymj.2011.12.001
76. Vadori R, Misra M, Mohanty AK (2016) Sustainable biobased blends from the reactive extrusion of polylactide and acrylonitrile butadiene styrene. J Appl Polym Sci 133(45):43771. doi:10.1002/app.43771
77. Hashima K, Nishitsuji S, Inoue T (2010) Structure-properties of super-tough PLA alloy with excellent heat resistance. Polymer 51(17):3934–3939. doi:10.1016/j.polymer.2010.06.045
78. Zhang C, Wang W, Huang Y, Pan Y, Jiang L, Dan Y, Luo Y, Peng Z (2013) Thermal, mechanical and rheological properties of polylactide toughened by expoxidized natural rubber. Mater Des 45:198–205. doi:10.1016/j.matdes.2012.09.024
79. Bouzouita A, Samuel C, Notta-Cuvier D, Odent J, Lauro F, Dubois P, Raquez JM (2016) Design of highly tough poly(l-lactide)-based ternary blends for automotive applications. J Appl Polym Sci 133(19):43402. doi:10.1002/app.43402
80. Taib RM, Ghaleb ZA, Mohd Ishak ZA (2012) Thermal, mechanical, and morphological properties of polylactic acid toughened with an impact modifier. J Appl Polym Sci 123(5):2715–2725. doi:10.1002/app.34884
81. Lemmouchi Y, Murariu M, Dos Santos AM, Amass AJ, Schacht E, Dubois P (2009) Plasticization of poly(lactide) with blends of tributyl citrate and low molecular weight poly(D,L-lactide)-b-poly(ethylene glycol) copolymers. Eur Polym J 45(10):2839–2848. doi:10.1016/j.eurpolymj.2009.07.006
82. Graham T (1864) On the molecular mobility of gases. J Chem Soc London 17:334–339
83. Duda JL, Zielinski JM (1996) Free volume theory. In: Neogi P (ed) Diffusion in polymers, vol 32. Marcel Dekker, New York, pp. 143–171
84. Theodorou DN (1996) Molecular simulations of sorption and diffusion in amorphous polymers. In: Neogi P (ed) Diffusion in polymers, vol 32. Marcel Dekker, New York, pp. 67–142

85. Xi L, Shah M, Trout BL (2013) Hopping of water in a glassy polymer studied via transition path sampling and likelihood maximization. J Phys Chem B 117(13):3634–3647
86. Siracusa V, Rocculi P, Romani S, Dalla Rosa M (2008) Biodegradable polymers for food packaging: a review. Trends Food Sci Technol 19(12):634–643. doi:10.1016/j.tifs.2008.07.003
87. Sorrentino A, Gorrasi G, Vittoria V (2007) Potential perspectives of bio-nanocomposites for food packaging applications. Trends Food Sci Technol 18:84–95
88. Rhim JW, Park HM, Ha CS (2013) Bio-nanocomposites for food packaging applications. Prog Polym Sci 38(10–11):1629–1652. doi:10.1016/j.progpolymsci.2013.05.008
89. Arrnentano I, Bitinis N, Fortunati E, Mattioli S, Rescignano N, Verdejo R, Lopez-Manchado MA, Kenny JM (2013) Multifunctional nanostructured PLA materials for packaging and tissue engineering. Prog Polym Sci 38(10–11):1720–1747. doi:10.1016/j.progpolymsci.2013.05.010
90. Lange J, Wyser Y (2003) Recent innovations in barrier technologies for plastic packaging—a review. Packag Technol Sci 16(4):149–158. doi:10.1002/pts.621
91. Pauly S (1999) Permeability and diffusion data. In: Brandrup J, Immergut EH, Grulke EA (eds) Polymer handbook, vol 2. Wiley, New York, pp. 543–569
92. Domenek S, Courgneau C, Ducruet V (2011) Characteristics and applications of PLA. In: Kalia S, Averous L (eds) Biopolymers: biomedical and environmental applications. Wiley, Hoboken/Scrivener, Salem, pp. 183–223
93. Mensitieri G, Di Maio E, Buonocore G, Nedi I, Oliviero M, Sansone L, Iannace S (2010) Processing and shelf life issues of selected food packaging materials and structures from renewable resources. Trends Food Sci Technol 22:72–80. doi:10.1016/j.tifs.2010.10.001
94. Martino VP, Jiménez A, Ruseckaite RA (2009) Processing and characterization of poly(lactic acid) films plasticized with commercial adipates. J Appl Polym Sci 112:2010–2018
95. Ambrosio-Martin J, Fabra MJ, Lopez-Rubio A, Lagaron JM (2014) An effect of lactic acid oligomers on the barrier properties of polylactide. J Mater Sci 49(8):2975–2986. doi:10.1007/s10853-013-7929-x
96. Sanchez-Garcia MD, Gimenez E, Lagaron JM (2007) Novel pet nanocomposites of interest in food packaging applications and comparative barrier performance with biopolyester nanocomposites. J Plast Film Sheet 23(2):133–148. doi:10.1177/8756087907083590
97. Belard L, Poncin-Epaillard F, Dole P, Averous L (2013) Plasma-polymer coatings onto different biodegradable polyesters surfaces. Eur Polym J 49(4):882–892. doi:10.1016/j.eurpolymj.2012.11.022
98. Lagaron JM, Sanchez G (2008) Thermoplastic nanobiocomposites for rigid and flexible food packaging applications. In: Chiellini E (ed) Environmentally compatible food packaging. Woodhead Publishing, Cambridge, pp. 62–89
99. Dong T, Yu ZF, Wu JX, Zhao ZL, Yun XY, Wang Y, Jin Y, Yang JJ (2015) Thermal and barrier properties of stretched and annealed polylactide films. Polym Sci Ser A 57(6):738–746. doi:10.1134/s0965545x15060073
100. Colomines G, Ducruet V, Courgneau C, Guinault A, Domenek S (2010) Barrier properties of poly(lactic acid) and its morphological changes induced by aroma compound sorption. Polym Int 59(6):818–826. doi:10.1002/pi.2793
101. Drieskens M, Peeters R, Mullens J, Franco D, Lemstra PJ, Hristova-Bogaerds DG (2009) Structure versus properties relationship of poly(lactic acid). I. Effect of crystallinity on barrier properties. J Polym Sci B Polym Phys 47(22):2247–2258
102. Guinault A, Sollogoub C, Ducruet V, Domenek S (2012) Impact of crystallinity of poly(lactide) on helium and oxygen barrier properties. Eur Polym J 48(4):779–788
103. Sawada H, Takahashi Y, Miyata S, Kanehashi S, Sato S, Nagai K (2010) Gas transport properties and crystalline structure of poly(lactic acid) membranes. Trans Mater Res Soc Jpn 35:241–246

104. Kanehashi S, Kusakabe A, Sato S, Nagai K (2010) Analysis of permeability; solubility and diffusivity of carbon dioxide; oxygen; and nitrogen in crystalline and liquid crystalline polymers. J Membr Sci 365(1–2):40–51. doi:10.1016/j.memsci.2010.08.035
105. Bai HW, Huang CM, Xiu H, Zhang Q, Deng H, Wang K, Chen F, Fu Q (2014) Significantly improving oxygen barrier properties of polylactide via constructing parallel-aligned Shish-Kebab-like crystals with well-interlocked boundaries. Biomacromolecules 15(4):1507–1514. doi:10.1021/bm500167u
106. Wen X, Zhang KY, Wang Y, Han LJ, Han CY, Zhang HL, Chen S, Dong LS (2011) Study of the thermal stabilization mechanism of biodegradable poly(L-lactide)/silica nanocomposites. Polym Int 60(2):202–210. doi:10.1002/pi.2927
107. Picard E, Espuche E, Fulchiron R (2011) Effect of an organo-modified montmorillonite on PLA crystallization and gas barrier properties. Appl Clay Sci 53(1):58–65. doi:10.1016/j.clay.2011.04.023
108. Li H, Huneault MA (2007) Effect of nucleation and plasticization on the crystallization of poly(lactic acid). Polymer 48:6855–6866
109. Wijmans JG, Baker RW (1995) The solution-diffusion model: a review. J Membr Sci 107(1-2):1–21
110. Choudalakis G, Gotsis AD (2009) Permeability of polymer/clay nanocomposites: A review. Eur Polym J 45(4):967–984. doi:10.1016/j.eurpolymj.2009.01.027
111. Paul MA, Alexandre M, Degee P, Henr'ist C, Rulmont A, Dubois P (2003) New nanocomposite materials based on plasticized poly(L-lactide) and organo-modified montmorillonites: thermal and morphological study. Polymer 44(2):443–450. doi:10.1016/s0032-3861(02)00778-4
112. Chang J-H, An YU, Sur GS (2003) Poly(lactic acid) nanocomposites with various organoclays. I. Thermomechanical properties, morphology, and gas permeability. J Polym Sci B Polym Phys 41(1):94–103
113. Sinha Ray S, Yamada K, Okamoto M, Ogami A, Ueda K (2003) New polylactide/layered silicate nanocomposites. III. High-performance biodegradable materials. Chem Mater 15(7):1456–1465
114. Zenkiewicz M, Richert J (2008) Permeability of polylactide nanocomposite films for water vapour, oxygen and carbon dioxide. Polym Test 27:835–840
115. Guo YC, Yang K, Zuo XH, Xue Y, Marmorat C, Liu Y, Chang CC, Rafailovich MH (2016) Effects of clay platelets and natural nanotubes on mechanical properties and gas permeability of poly (lactic acid) nanocomposites. Polymer 83:246–259. doi:10.1016/j.polymer.2015.12.012
116. Ortenzi MA, Basilissi L, Farina H, Di Silvestro G, Piergiovanni L, Mascheroni E (2015) Evaluation of crystallinity and gas barrier properties of films obtained from PLA nanocomposites synthesized via "in situ" polymerization of L-lactide with silane-modified nanosilica and montmorillonite. Eur Polym J 66:478–491. doi:10.1016/j.eurpolymj.2015.03.006
117. Ambrosio-Martin J, Lopez-Rubio A, Fabra MJ, Lopez-Manchado MA, Sorrentino A, Gorrasi G, Lagaron JM (2016) Synergistic effect of lactic acid oligomers and laminar graphene sheets on the barrier properties of polylactide nanocomposites obtained by the in situ polymerization pre-incorporation method. J Appl Polym Sci 133(2). doi:10.1002/app.42661
118. Pinto AM, Cabral J, Pacheco Tanaka DA, Mendes AM, Magalhaes FD (2013) Effect of incorporation of graphene oxide and graphene nanoplatelets on mechanical and gas permeability properties of poly(lactic acid) films. Polym Int 62(1):33–40. doi:10.1002/pi.4290
119. Tripathi N, Katiyar V (2016) PLA/functionalized-gum arabic based bionanocomposite films for high gas barrier applications. J Appl Polym Sci 133(21):43458. doi:10.1002/app.43458
120. Azizi S, My AS, Alloin F, Dufresne A (2005) Review of recent research into cellulosic whiskers, their properties and their application in nanocomposite field. Biomacromolecules 6(2):612–626

121. Espino-Perez E, Bras J, Ducruet V, Guinault A, Dufresne A, Domenek S (2013) Influence of chemical surface modification of cellulose nanowhiskers on thermal, mechanical, and barrier properties of poly(lactide) based bionanocomposites. Eur Polym J 49(10):3144–3154. doi:10.1016/j.eurpolymj.2013.07.017
122. Espino-Perez E, Domenek S, Belgacem N, Sillard C, Bras J (2014) Green process for chemical functionalization of nanocellulose with carboxylic acids. Biomacromolecules 15(12):5441–4560. doi:10.1021/bm5013458
123. Espino-Perez E, Gilbert RG, Domenek S, Brochier-Salon MC, Belgacem MN, Bras J (2016) Nanocomposites with functionalised polysaccharide nanocrystals through aqueous free radical polymerisation promoted by ozonolysis. Carbohydr Polym 135:256–266. doi:10.1016/j.carbpol.2015.09.005
124. Sanchez-Garcia M, Lagaron J (2010) On the use of plant cellulose nanowhiskers to enhance the barrier properties of polylactic acid. Cellulose 17(5):987–1004
125. Sanchez-Garcia MD, Gimenez E, Lagaron JM (2008) Morphology and barrier properties of solvent cast composites of thermoplastic biopolymers and purified cellulose fibers. Carbohydr Polym 71(2):235–244. doi:10.1016/j.carbpol.2007.05.041
126. Fukuzumi H, Saito T, Wata T, Kumamoto Y, Isogai A (2009) Transparent and high gas barrier films of cellulose nanofibers prepared by TEMPO-mediated oxidation. Biomacromolecules 10(1):162–165. doi:10.1021/bm801065u
127. Martucci JF, Ruseckaite RA (2010) Three-layer sheets based on gelatin and poly(lactic acid), part 1: preparation and properties. J Appl Polym Sci 118(5):3102–3110. doi:10.1002/app.32751
128. Svagan AJ, Akesson A, Cardenas M, Bulut S, Knudsen JC, Risbo J, Plackett D (2012) Transparent films based on PLA and montmorillonite with tunable oxygen barrier properties. Biomacromolecules 13(2):397–405. doi:10.1021/bm201438m
129. Liu RYF, Ranade AP, Wang HP, Bernal-Lara TE, Hiltner A, Baer E (2005) Forced assembly of polymer nanolayers thinner than the interphase. Macromolecules 38(26):10721–10727. doi:10.1021/ma051649x
130. Oliveira NS, Dorgan J, Coutinho JAP, Ferreira A, Daridon JL, Marrucho IM (2007) Gas solubility of carbon dioxide in poly(lactic acid) at high pressures: thermal treatment effect. J Polym Sci B Polym Phys 45(5):616–625
131. Bao L, Dorgan JR, Knauss D, Hait S, Oliveira NS, Maruccho IM (2006) Gas permeation properties of poly(lactic acid) revisited. J Membr Sci 285(1–2):166–172. doi:10.1016/j.memsci.2006.08.021
132. Dorgan JR, Lehermeier HJ, Palade L-I, Cicero J (2001) Polylactides: properties and prospects of an environmentally benign plastic from renewable resources. Macromol Symp 175:55–66
133. Lehermeier HJ, Dorgan JR, Way JD (2001) Gas permeation properties of poly(lactic acid). J Membr Sci 190:243–251
134. Komatsuka T, Kusakabe A, Nagai K (2008) Characterization and gas transport properties of poly(lactic acid) blend membranes. Desalination 234(1–3):212–220
135. Sato S, Nyuui T, Matsuba G, Nagai K (2014) Correlation between interlamellar amorphous structure and gas permeability in poly(lactic acid) films. J Appl Polym Sci 131(16):40626. doi:10.1002/app.40626
136. Shogren R (1997) Water vapor permeability of biodegradable polymers. J Polym Environ 5(2):91–95
137. Siparsky G, Voorhees K, Dorgan J, Schilling K (1997) Water transport in polylactic acid (PLA), PLA/polycaprolactone copolymers, and PLA/polyethylene glycol blends. J Polym Environ 5(3):125–136
138. Holm VK, Ndoni S, Risbo J (2006) The stability of poly(lactic acid) packaging films as influenced by humidity and temperature. J Food Sci 71:E40–E44
139. Tsuji H, Okino R, Daimon H, Fujie K (2006) Water vapor permeability of poly(lactide)s: effects of molecular characteristics and cristallinity. J Appl Polym Sci 99:2245–2252

140. Auras R, Harte B, Selke S (2004) An overview of polylactides as packaging materials. Macromol Biosci 4:835–864
141. Tsuji H, Fukui I (2003) Enhanced thermal stability of poly(lactide)s in the melt by enantiomeric polymer blending. Polymer 44(10):2891–2896. doi:10.1016/s0032-3861(03)00175-7
142. Davis EM, Minelli M, Baschetti MG, Elabd YA (2013) Non-Fickian diffusion of water in polylactide. Ind Eng Chem Res 52(26):8664–8673. doi:10.1021/ie302342m
143. Rhim J-W, Hong S-I, Ha C-S (2009) Tensile, water vapor barrier and antimicrobial properties of PLA/nanoclay composite films. LWT Food Sci Technol 42(2):612–617
144. Delpouve N, Delbreilh L, Stoclet G, Saiter A, Dargent E (2014) Structural dependence of the molecular mobility in the amorphous fractions of polylactide. Macromolecules 47(15): 5186–5197. doi:10.1021/ma500839p
145. Tsuji H, Tsuruno T (2010) Water vapor permeability of poly(L-lactide)/poly(D-lactide) stereocomplexes. Macromol Mater Eng 295(8):709–715. doi:10.1002/mame.201000071
146. Liu D, Li HL, Zhou GX, Yuan ML, Qin YY (2015) Biodegradable poly(lactic-acid)/poly (trimethylene-carbonate)/laponite composite film: development and application to the packaging of mushrooms (*Agaricus bisporus*). Polym Adv Technol 26(12):1600–1607. doi:10.1002/pat.3587
147. Halasz K, Hosakun Y, Csoka L (2015) Reducing water vapor permeability of poly(lactic acid) film and bottle through layer-by-layer deposition of green-processed cellulose nanocrystals and chitosan. Int J Polym Sci 2015:1–6. doi:10.1155/2015/954290
148. Auras R, Harte B, Selke S (2006) Sorption of ethyl acetate and d-limonene in poly(lactide) polymers. J Sci Food Agric 86(4):648–656
149. Haugaard V, Weber C, Danielsen B, Bertelsen G (2002) Quality changes in orange juice packed in materials based on polylactate. Eur Food Res Technol 214(5):423–428
150. Mauricio-Iglesias M, Peyron S, Chalier P, Gontard N (2011) Scalping of four aroma compounds by one common (LDPE) and one biosourced (PLA) packaging materials during high pressure treatments. J Food Eng 10:9–15
151. Salazar R, Domenek S, Courgneau C, Ducruet V (2012) Plasticization of poly(lactide) by sorption of volatile organic compounds at low concentration. Polym Degrad Stab 97(10): 1871–1880
152. Salazar R, Domenek S, Ducruet V (2014) Interactions of flavoured oil in-water emulsions with polylactide. Food Chem 148:138–146
153. Jin Z, Tian Y, Wang Y (2010) Chemistry and thermodynamics properties of lactic acid and lactide and solvent miscibility. In: Auras R, Lim LT, Selke S, Tsuji H (eds) Poly(lactic acid): synthesis, structures, properties, processing, and applications. Wiley, Hoboken, pp. 19–25
154. Widiastuti I, Sbarski I, Masood SH (2014) Mechanical response of poly(lactic acid)-based packaging under liquid exposure. J Appl Polym Sci 131(16):40600. doi:10.1002/app.40600